1993

An optical technique for the measurement of two-dimensional texture of roller bearing surfaces.

Wai-Hong. Wong
University of Windsor

NOTICE

AVIS

The quality of this microform is heavily dependent upon the quality of the original thesis submitted for microfilming. Every effort has been made to ensure the highest quality of reproduction possible.

If pages are missing, contact the university which granted the degree.

Some pages may have indistinct print especially if the original pages were typed with a poor typewriter ribbon or if the university sent us an inferior photocopy.

Reproduction in full or in part of this microform is governed by the Canadian Copyright Act, R.S.C. 1970, c. C-30, and subsequent amendments.

La qualité de cette microforme dépend grandement de la qualité de la thèse soumise au microfilmage. Nous avons tout fait pour assurer une qualité supérieure de reproduction.

S'il manque des pages, veuillez communiquer avec l'université qui a conféré le grade.

La qualité d'impression de certaines pages peut laisser à désirer, surtout si les pages originales ont été dactylographiées à l'aide d'un ruban usé ou si l'université nous a fait parvenir une photocopie de qualité inférieure.

La reproduction, même partielle, de cette microforme est soumise à la Loi canadienne sur le droit d'auteur, SRC 1970, c. C-30, et ses amendements subséquents.

Canada

AN OPTICAL TECHNIQUE FOR THE MEASUREMENT
OF
2-D TEXTURE OF ROLLER BEARING SURFACES

by

Wai-Hong Wong

A Thesis
Submitted to
the Faculty of Graduate Studies and Research
Through
the Department of Mechanical Engineering
in Partial Fulfillment of the Requirements for
the Degree of Master of Applied Science at
the University of Windsor

Windsor, Ontario, Canada
1993

The author has granted an irrevocable non-exclusive licence allowing the National Library of Canada to reproduce, loan, distribute or sell copies of his/her thesis by any means and in any form or format, making this thesis available to interested persons.

L'auteur a accordé une licence irrévocable et non exclusive permettant à la Bibliothèque nationale du Canada de reproduire, prêter, distribuer ou vendre des copies de sa thèse de quelque manière et sous quelque forme que ce soit pour mettre des exemplaires de cette thèse à la disposition des personnes intéressées.

The author retains ownership of the copyright in his/her thesis. Neither the thesis nor substantial extracts from it may be printed or otherwise reproduced without his/her permission.

L'auteur conserve la propriété du droit d'auteur qui protège sa thèse. Ni la thèse ni des extraits substantiels de celle-ci ne doivent être imprimés ou autrement reproduits sans son autorisation.

ISBN   0-315-87356-6

Canada

ABSTRACT

An optical method based on the laser light scattering technique for surface roughness measurement of tapered roller bearings was developed. This technique was based on an analysis of the Bi-directional Reflective Distribution Function (BRDF) of the scattering pattern from a bearing surface.

A He-Ne laser ($\lambda = 0.6328$ μm) was used as a coherent light source to illuminate the surface of the roller bearings. They were surface-ground and honed to obtain 1-D and 2-D surface texture in order to improve lubrication. The scattering pattern was captured by a CCD camera and then digitized by a frame grabber board on a PC-AT computer for analysis. The BRDF of the scattering pattern was obtained in order to derive the zero and second moments. These were used as the optical roughness parameters of the surface and then correlated to the mechanical root mean square (RMS) roughness and the RMS slope of the surface profile which were obtained from a stylus instrument.

Correlation curves of the zero moment versus the RMS roughness and the second moment versus the RMS slope of 1-D and 2-D surface texture roller bearings were obtained separately. Good correlations were observed, and the curves showed the relationship between the optical roughness parameters and the mechanical roughness parameters. The normalized zero and second moments correlation curves were also obtained and these curves for 1-D and 2-D surface texture roller bearings coincided.

The possible error of this optical measurement technique was determined to be less than 10%.

Dedicated to
my parents, sister and brother

ACKNOWLEDGEMENTS

TABLE OF CONTENTS

LIST OF FIGURES

LIST OF TABLES

NOMENCLATURE

a = width of the slit

A = unit illuminated area on a surface

d = path difference

d_x, d_y = spatial distances of the scattering pattern

E = amplitude of the diffraction pattern in the far field

E_T = total light source amplitude

f = spatial frequency

f_d = fundamental frequency

f_x = spatial frequency in x-direction

f_y = spatial frequency in y-direction

g(x) = a spatial domain function

G(f) = a frequency domain function

h = height variations of a surface

i = a positive integer

$I(f_x, f_y)$ = greylevel intensity of the scattering pattern

I_i = intensity of the incident beam

I(r) = average intensity

I_s = intensity of the scattering beam

k = a positive integer

l = focal length of the transform lens

L = assessment length

m = root mean square slope (RMS slope)

M = magnification of the system

M_0 = zero moment

M_2 = second moment

M_0' = zero moment of the scattering pattern greylevel intensity

M_2' = second moment of the scattering pattern greylevel intensity

n = integer indicating the order

P_{ave} = distance average roughness power

P_i = light flux of incident beam

P_s = light flux of scattering beam

Q = a dimensionless factor related to the surface material property

r_p, r_p = the ratio of the complex reflection coefficients for the P and S-component of the electromagnetic field

R_a = average roughness

R_t = maximum peak to valley height

$S(f_x, f_y)$ = surface power spectral density

SD = standard deviation of intensity

t_o = height of the slit function

T = a finite spatial distance

T(u) = optical Fourier transform of the slit function

u = frequency domain of the optical Fourier transform of the slit function

V = normalized average contrast

x = spatial domain of the original wave front function

X_m = arithmetic mean of the data

$z(x)$ = height variations of a surface profile

$Z(f)$ = Fourier transform of the surface profile "z(x)"

α = an angle

$\gamma(x)$ = phase modulation function

Δ, Ψ = Ellipsometry parameters

θ = the angle between the normal and the direction of interest

θ_i, θ_1 = incident angle

θ_n = reflection angle of the order n

θ_s, θ_2 = scattering angle

θ_3 = angle of lateral scattering

λ = illumination wavelength

Λ = wavelength of a periodic surface

σ = root mean square roughness (RMS roughness)

Φ = phase difference between the first and the Nth source in a slit

Φ_s = angle of lateral scattering

Ω = solid angle

$\mathcal{F}[\ ]$ = Fourier transform

CHAPTER I

INTRODUCTION

There is an increasing in awareness of the importance of the surface texture of machined tools in production and manufacturing industries. Surface texture is important for applications involving contact surfaces, either being stationary or in relative motion, for example, rolling or sliding. For a press fit, roughness is required for maintaining a certain amount of friction. On the other hand, to reduce friction, the roughness has to be reduced to a minimum. For lubrication, a certain roughness and texture are needed to distribute and retain the lubricant over the surface of interest. In die casting or plastic injection molding, smoothness is required for optical components, for example. Surface texture also indicates tool and machine tool conditions, for example, roughness in turning relates to cutter geometry. Chatter marks or form errors can be related to the movement of the tool and work-piece which in turn reflects the condition of the machine. Therefore, a need exists for the development of sensors for measuring the texture of the machined parts

Production industries require on-line or in-process surface texture measurement techniques for quality control and condition monitoring. These techniques must provide a fast measurement process. The traditional stylus instrument provides a low speed contact measurement method which is not an on-line, in-process roughness measurement technique. On the other hand, many non-contact techniques exist for surface texture measurements such as magnetic, capacitance, ultrasonic, etc. Among these, the optical

technique seems to offer the best advantages because the optical technique can provide high speed as well as a high resolution measurement of surfaces and can measure an area rather than a line on surfaces. Also, the optical technique works properly even if the stand-off distance from the surface is large. Therefore, the optical technique is the most promising for high speed, 2-D texture measurement and this will be considered in the next chapter.

In this section, a description of the surface texture will be given. A review of methods for surface texture assessment follows.

1.1 Surface Texture

According to the American National Standards Institute [ANSI, 1978], surface texture is composed of the repetitive or random deviations from the nominal surface which form the three dimensional topography of the surface. Surface texture components include lay, waviness, roughness (Figure 1.1).

1) Lay: This involves the machine feed marks left on the surface by a cutting tool. The lay direction is defined with respect to the main edge of the part. A surface may have more than one lay direction created by a number of passes in different directions of the cutting tool.

2) Waviness: This is the long wavelength of the surface. Waviness may result from machine or work deflections, vibrations, chatter, etc.

3) Roughness : These are the finer irregularities of the surface texture. Roughness usually results from the inherent action of the production process. A single point cutting tool, for example, is dependent on the tool geometry and the feed. A common parameter for

2

characterizing roughness is the average roughness (R_a) of the surface profile. The average roughness is the arithmetic mean of the absolute value of the height variations on the surface (Figure 1.2). Mathematically it can be expressed as :

$$R_a = \frac{1}{L} \int_0^L |z(x)| \, dx \qquad (1.1)$$

where L = assessment length,

z(x) = height variations of the surface profile.

Other commonly used surface roughness parameters include R_t & RMS. R_t is the maximum peak to valley height of the surface profile and RMS is the root mean square roughness (RMS roughness) which will be described in section 3.4.

4) Flaws : These are unintentional irregularities which occur infrequently or at wildly varying intervals and do not have any consistent pattern. Flaws include scratches, cracks, dents, blowholes, etc.

1.2 Contact and Non-Contact Roughness Measurement

Surface texture measurement techniques can be classified into two types: contact and non-contact techniques.

a) Contact Method

The traditional way of measuring roughness is by the mechanical stylus instrument. This device is equipped with a diamond tip stylus for tracing the surface of interest. The output voltage of this device is proportional to the height variations of the surface profile being measured. This measurement method has several disadvantages :

1) The stylus instrument can only measure along one single line.

3

2) It is a relatively slow measurement process for surface measurement and cannot be adopted for high-speed measurement in a production line.

3) Soft surfaces may be damaged by the stylus which may affect the quality of the products.

Despite these drawbacks, the mechanical stylus instrument is still the most commonly used instrument for surface roughness measurement in production industries and the roughness standards are normally defined in terms of the stylus measurements.

b) Non-Contact Method

There are several non-contact surface roughness measurement methods such as optical, ultra-sonic [Tenoudji, 1982 ; Blessing, 1988], and capacitance techniques [Garbini, 1985]. Optical techniques are more favourable because of the following advantages:

1) The process is capable of area measurement. Thus, it can be applied to surfaces of 2-D texture.

2) As it provides measurements on a surface area, it is capable of fast speed which is one of the requirements for on-line measurement.

3) The technique is rugged and is not affected by electrical noise.

A detailed review of the optical techniques is given in chapter II.

1.3 Objectives

Certain textures are distributed over the surfaces of roller bearings for the purpose of friction reduction and lubrication. These textures can be two-dimensional for better performance or other uses. Therefore, it is necessary to develop a surface texture

4

measurement technique for roller bearings during manufacturing. Due to the advantages of the optical technique described in the previous section, it is considered to be the appropriate roughness measurement technique for 2-D texture of roller bearings. The main objectives for the work presented in this research are as follows:

1) To develop an optical measurement technique for the assessment of 2-D surface texture using the Bi-directional Reflective Distribution Function (BRDF) of the scattering pattern from bearing surfaces.

2) To derive optical parameter(s) that can be related to the mechanical roughness of this type of surface.

3) To obtain a correlation between the optical roughness parameter(s) and the mechanical roughness parameter(s) for roller bearings having 2-D surface texture.
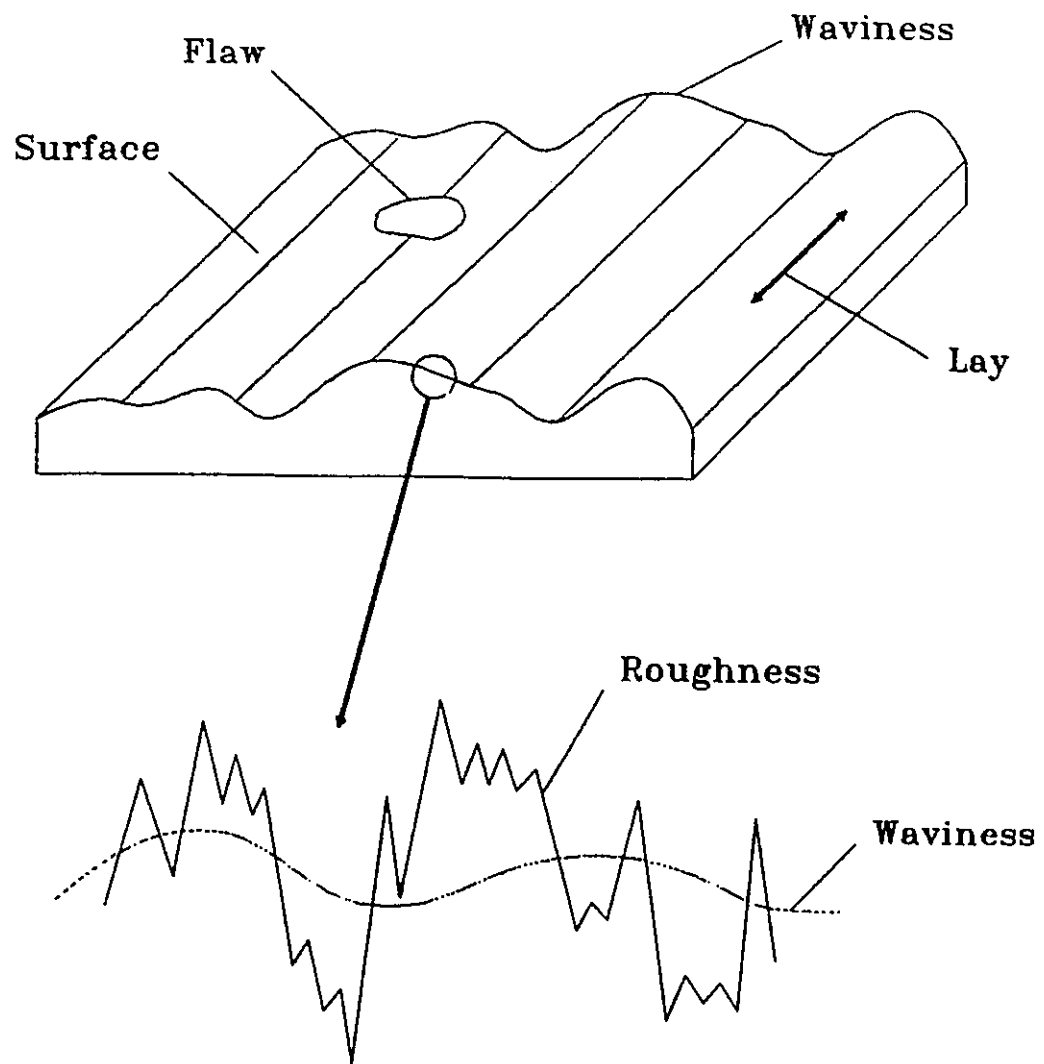
Figure 1.1 Different components of surface texture
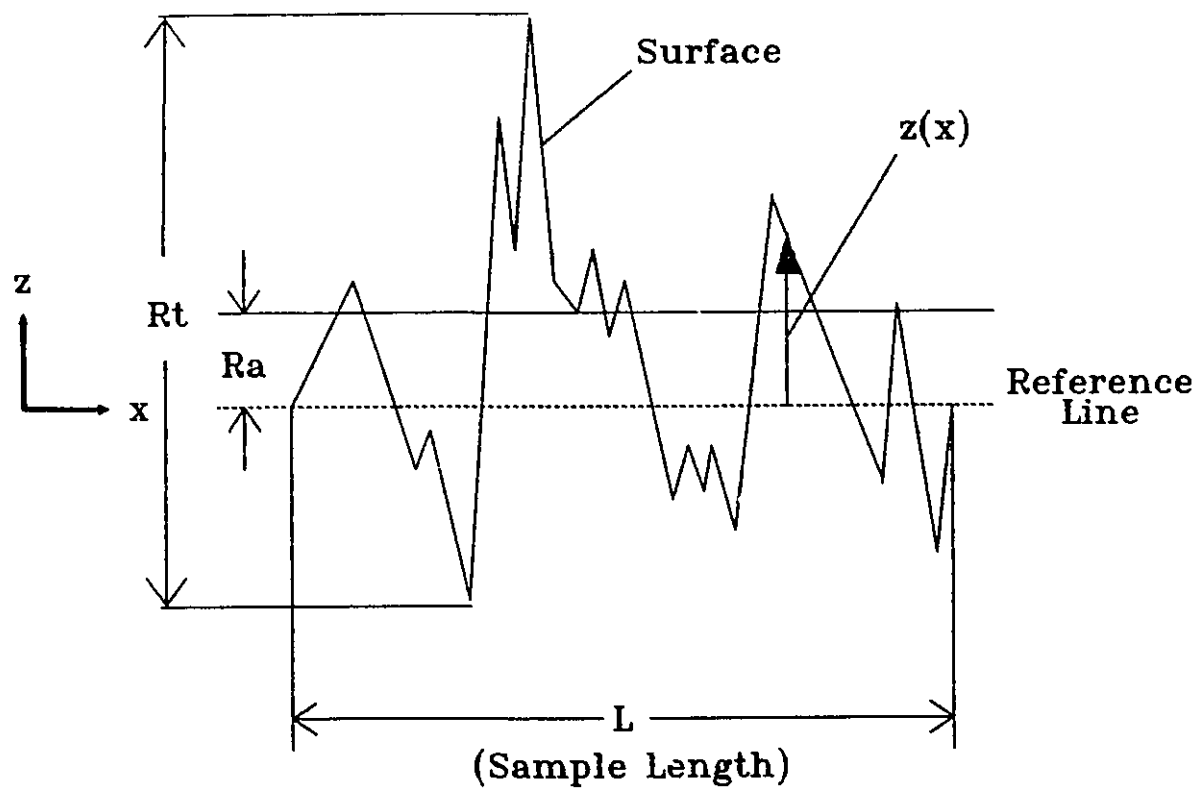
Figure 1.2   Description of Ra and Rt

CHAPTER II

LITERATURE SURVEY OF OPTICAL TECHNIQUES

Optical techniques were developed primarily as an alternative to overcome some of the disadvantages in contact surface roughness measurement methods. These techniques are capable of being adapted for an on-line, in-process surface roughness measurement method for industrial use. These optical techniques can be grouped according to the physical phenomena on which the measuring system is based. As such, they are classified into some broad categories such as interferometric methods, laser speckle, optical Fourier transform and light scattering. In this chapter, a review of these optical measurement methods is given.

2.1 Interferometric

Interferometry is adopted for use in the measurement of very smooth surfaces in laboratories. In this technique, interference fringes are created and used to quantify the height of surface irregularity. A schematic diagram of the set-up for this technique is shown in Figure 2.1.

A monochromatic light source, such as a He-Ne laser, projects the light through a reference optical flat and then onto the sample surface. The reflected light beams from the reference optical flat and from the sample surface are combined to form fringes. Dark fringes (minimum light intensity) will occur at the location where the path difference between the two beams is a multiple of half of the illumination wavelength. Similarly,

bright fringes (maximum light intensity) will occur where the path difference is a multiple of the wavelength. If the sample surface is slightly tilted relative to the reference surface, a set of parallel fringes will form. Any distortion in the fringe pattern can be related to the surface deviation from the reference. The fringe pattern is focused through a microscope optical system onto the image plane of a CCD camera. The patterns can then be captured, digitized and processed to give the surface profile of the sample surface. Due to its high resolution, this technique can measure a surface as smooth as 1 nm RMS roughness value. The measured maximum roughness in this case is limited to less than $\lambda/2$. At this roughness, the interference fringes will merge together.

There are several commercially available surface roughness measurement systems that are based on interferometry [Hariharan, 1985]. For example, the oblique incidence interferometry can measure surfaces having low reflectivity. This measurement is carried out by using an oblique incident light in conjunction with a reference surface made of fine-ground glass or metal. Zygo [Sommargren, 1981] manufactures Heterodyne interferometry, another class of interferometric roughness measurement systems. It uses a two frequency laser beam and sophisticated phase detecting electronics to give a vertical sensitivity in the order of one Angstrom. Other important interferometric measurement methods include holographic interferometry. This measuring system determines the variation in surface height by comparing the stored interfering wavefronts (in the form of a hologram) with another wavefront. This method allows us to also measure accurately any change in the shape of the surface.

The interferometric techniques are, in general, applicable to very smooth surfaces. Furthermore, they are very sensitive to temperature change, air movement and building

vibration. Thus they cannot be used on production floor, especially for on-line, in-process surface roughness measurement.

2.2 Laser Speckle

This technique utilizes the speckle phenomenon that occurs when a coherent light is reflected from a surface. A schematic diagram of the apparatus used by Fujii [1977] and Asakura [1978] is shown in Figure 2.2. In this set-up, a folding mirror directs a He-Ne laser beam to an inverted telescope. The expanded light beam is filtered through an aperture and then focused onto a small area of the surface by a lens. A random speckle pattern, consisting of dark and bright regions, forms at the image plane in the far field. A photo-multiplier with a small pinhole is placed at the image plane to measure the intensity of the pattern. A varying signal is obtained when the sample is traversed at a constant speed. The signal is then used to determine the speckle contrast via the equation:

$$V = \frac{SD}{I(r)} = \frac{\sqrt{I^2(r) - [I(r)]^2}}{I(r)} \qquad (2.1)$$

where V = normalized average contrast,

SD = standard deviation of intensity,

I(r) = average intensity.

This calculated contrast value can then be correlated to mechanical roughness parameters such as average roughness (R_a) or RMS roughness. As the speckle is related to the degree of randomness in the surface, the smaller the contrast, the greater the roughness. Correlation curves are different for different materials and different machining processes. The upper roughness limit for this technique is determined by the illumination wavelength

λ. In practice, this value is found to be less than about 0.1 λ. Therefore, this technique is not applicable to relatively rough surfaces. It should also be mentioned that this technique only yields statistical averages of roughness. It is not possible to derive other data relating to any functional aspects of the surface such as R_t, or a bearing curve, etc. from a simple average speckle contrast.

2.3 Ellipsometry

This technique measures the change in the polarization state of a light beam when it is reflected from a surface [Azzam & Bashara, 1977]. Figure 2.3 shows a schematic diagram of an ellipsometer. The P-component is parallel to the plane of incidence and the S-component is perpendicular to the plane of incidence. The ratio of the complex reflection coefficients for the P-component (r_p) and the S-component (r_s) of the electromagnetic field is determined (r_p/r_s) and related to the ellipsometry parameters "Δ" & "Ψ" via equation 2.2 [Azzam & Bashara, 1977 ; Kruger & Hayfield, 1971] :

$$r_p/r_s = (\tan \Psi) \, e^{i\Delta} \qquad (2.2)$$

where tan Ψ is equal to the ratio of the P and S reflection coefficients and Δ is equal to the phase shift between them. These parameters can then be used with the Fresnel equations to calculate the optical constants of solids and can be related to the surface roughness.

Lonardo [1974 ; 1978] used the ellipsometric technique as an in-process surface roughness detection tool for ground and polished steel surfaces. Vorburger and Ludema

11

[1980] compared the ellipsometry parameters for lapped and ground surfaces with the roughness parameters measured by a stylus instrument. However, this technique cannot be used to measure the surface roughness of engineering surfaces directly because this technique is sensitive to the surface properties, such as damage or defect, and it is also sensitive to temperature.

2.4 Optical Fourier Transforms

The optical Fourier Transforms can be used to relate the diffraction pattern generated from a rough surface and its surface texture [Kurada, 1988 ; Cuthbert, 1991]. Examples of one- and two-dimensional diffraction patterns through a single slit are shown in Figures 2.4 a and b. The diffraction phenomenon through a single slit can be explained using the principle of physical optics. By Huygen's principle, the slit can be divided into a large number (N) of points and each point on the slit can be considered as a source. The waves generated from these sources form a wave front. The phase difference between the first and the Nth source can be expressed as:

$$\Phi = \frac{2\pi a \sin\theta}{\lambda} \qquad (2.3)$$

where Φ = phase difference between the first and the Nth source,

a = the width of the slit,

θ = the angle between the normal and the direction of interest,

λ = illumination wavelength.

In Figure 2.5, the arc of the small arrows shows the phasors representing the wave disturbances that reach point p on the screen of Fig. 2.4a. The amplitude "E" of the

12

diffraction pattern in the far field is given as [Halliday & Resnick, 1978]:

$$E = 2 r \sin(\Phi/2)$$

Φ can be expressed as:

$$\Phi = \frac{E_T}{r}$$

combining yields:

$$E = E_T \frac{\sin(\phi/2)}{(\phi/2)} = E_T \, sinc(\phi/2) \qquad (2.4)$$

where E_T = total light source amplitude.

The diffraction pattern of the slit can also be determined by a Fourier transform of a slit function (Figure 2.6). This transform is:

$$T(u) = \int_{-a/2}^{a/2} t_o e^{(-2\pi jux)} dx$$

$$= t_o a \frac{\sin \pi ua}{\pi ua} = t_o a \, sinc(\pi ua) \qquad (2.5)$$

where $T(u)$ = the optical Fourier transform of the slit function,

t_o = the height of the slit function,

a = the width of the slit,

u = frequency domain of the optical Fourier transform of the slit function,

x = spatial domain of the original wave front function.

13

By comparing equations (2.4) and (2.5), one can observe that they are equivalent. Thus the diffraction pattern of light through a single slit formed in the far field can be represented mathematically by the Fourier transform of the slit function.

The phenomenon of light diffraction from rough surfaces can be quantified by considering two light beams from the same coherent source incident on the rough surface as shown in Figure 2.7. A ray reflecting the rough surface will trace path (2) while the ray reflecting from the perfectly (imaginary) smooth surface will trace path (1). These two paths will meet at infinity (far field) and the intensity of the combined beam is determined by the phase difference of these two beams due to the height variations of the surface. The relationship between the phase and the surface height can be derived by considering the geometry in Figure 2.7.

The phase associated with a path difference d is given by:

$$\gamma(x) = \frac{2\pi d}{\lambda} \pm 2n\pi \qquad (2.6)$$

where $\gamma(x)$ = phase modulation function,

λ = the illumination wavelength,

n = a positive integer.

From Figure 2.7, the path difference is given by:

$$d = \Delta_1 + \Delta_2 \qquad (2.7)$$

For triangle ABD :

14

$$\Delta_1 = \frac{h}{\cos \alpha} \qquad (2.8)$$

For triangle ABC :

$$\Delta_2 = \Delta_1 \cos 2\alpha \qquad (2.9)$$

Substitute Equation (2.8) & (2.9) into Equation (2.7) and after reduction:

$$d = 2h\cos\alpha \qquad (2.7)$$

Equation (2.6) now becomes:

$$\gamma(x) = \frac{4\pi h \cos \alpha}{\lambda} \pm 2n\pi$$

When α is very small, the above equation is reduced to :

$$\gamma(x) = \frac{4\pi h}{\lambda} \pm 2n\pi$$

For a unique representation of $\gamma(x)$, the maximum of $\gamma(x)$ has to be less than 2π:

$$\frac{4\pi h}{\lambda} < 2\pi$$

$$\rightarrow \quad h < \lambda/2$$

15

Therefore, the surface height variation (h) measured by this technique is small compared with the illumination wavelength.

2.5 Light Scattering

The scattering of light from rough surfaces can be treated as the scattering of electromagnetic waves. Studies of electromagnetic wave scattering were first carried out by Beckmann and Spizzichino [1963]. When a beam of coherent light is reflected from a surface, the radiation is scattered into an angular distribution. If the surface is smooth, the scattering pattern is localized and concentrated around the specular direction (Figure 2.8a). As the roughness increases, the intensity of the specular beam decreases while the scattered radiation increases, i.e. the reflecting beam is more diffuse (Figure 2.8b). The distribution characteristics of the scatter can be studied and related to the roughness of the surface. Chandley [1976] estimated the auto-correlation functions obtained by a Hankel transform of the scattering patterns of rough surfaces. Brodmann, Rodenstock and Thurn [1984] related the power spectrum from the scattering patterns to the stylus measurements. Kurada [1988] correlated the normalized spectrum RMS to the average roughness (R_a) obtained by the stylus instrument. A detailed description of the light scattering methods will be given in Chapter III.
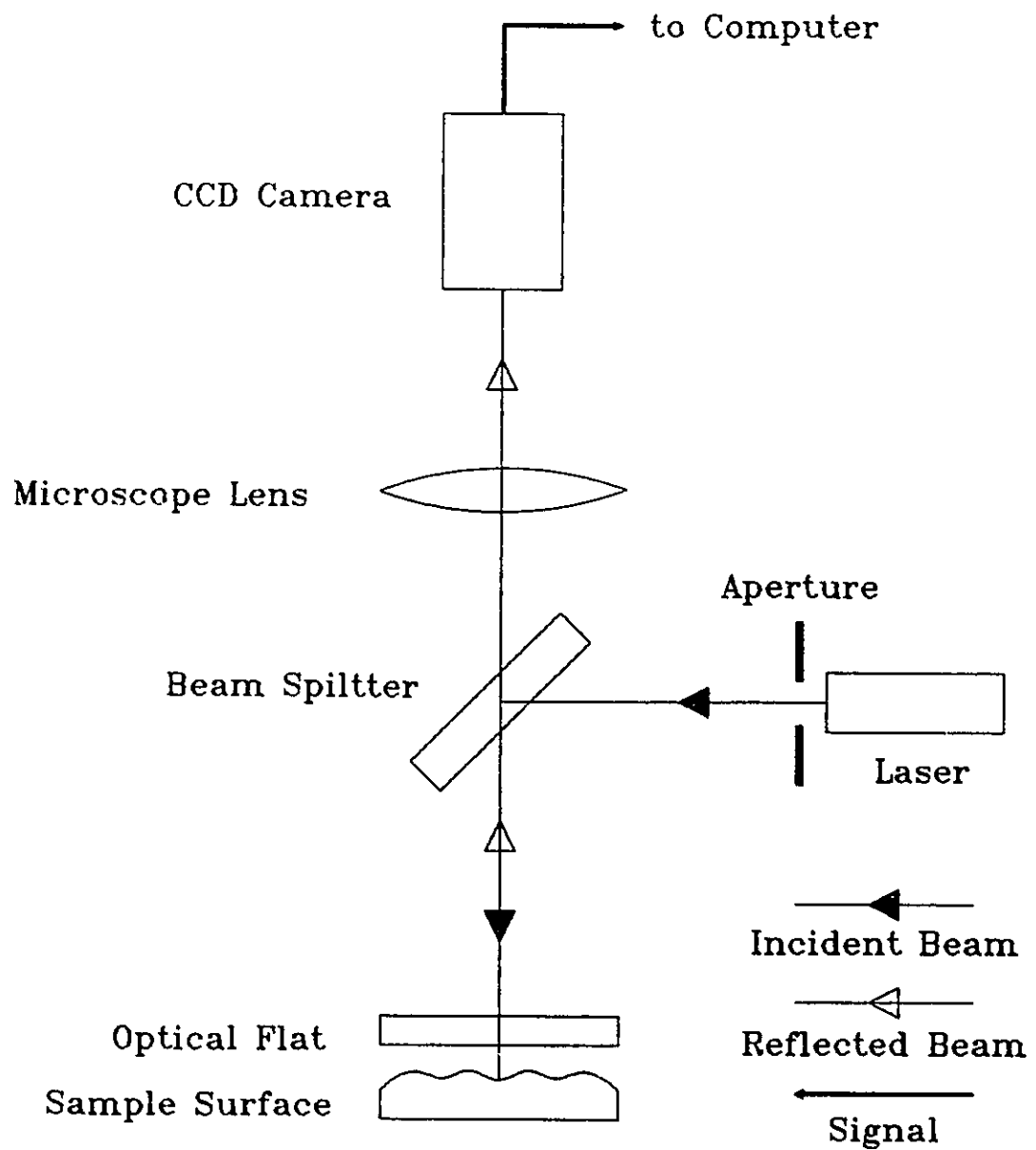
Figure 2.1 Schematic diagram of the setup for roughness
measurement using interferometric technique
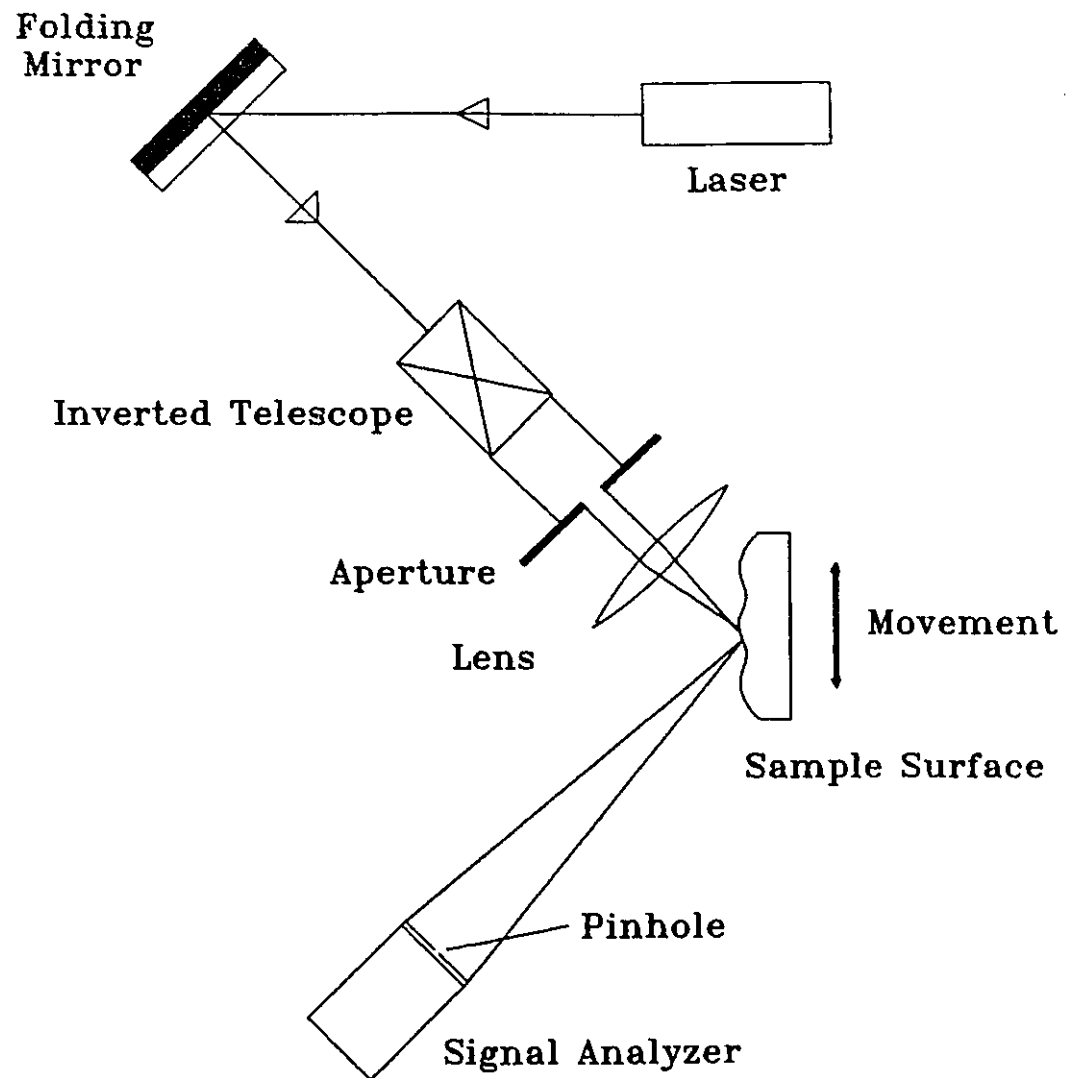
Figure 2.2   Schematic diagram of the setup for roughness
measurement using laser speckle
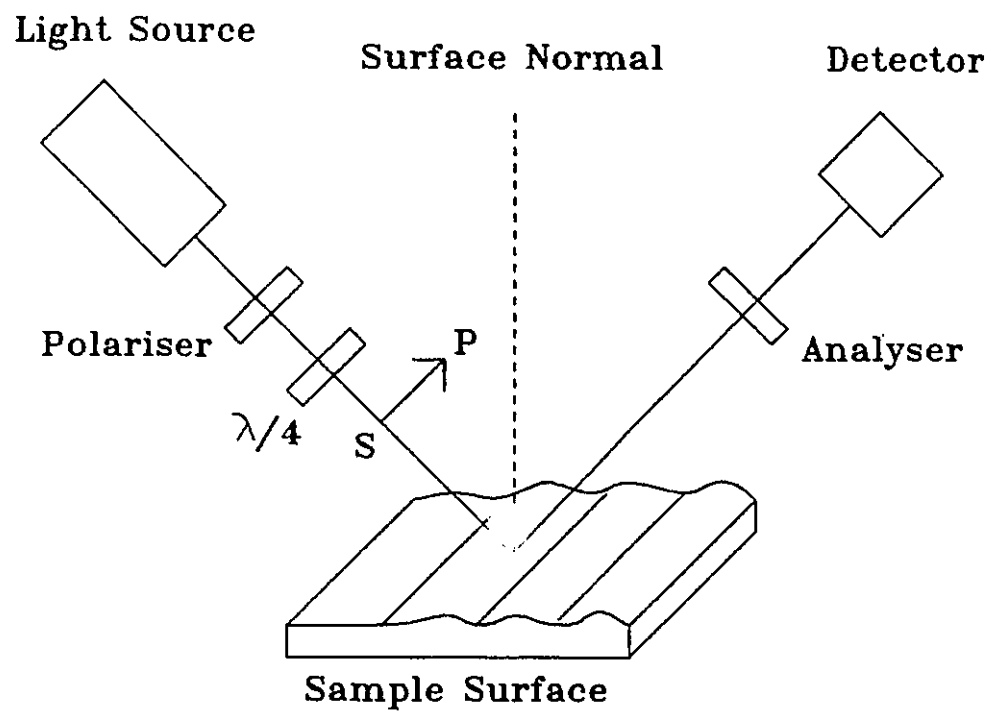
Figure 2.3 Schematic diagram of the setup for roughness
measurement using ellipsometry technique
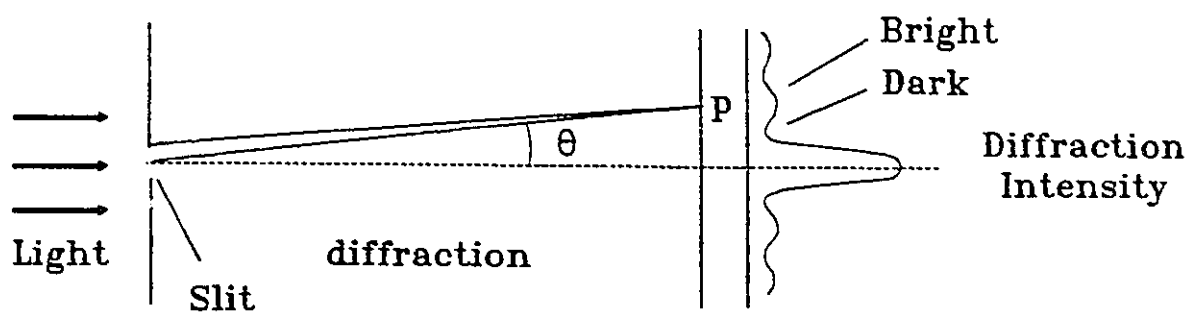
Figure 2.4a 1-D light diffraction through a single slit
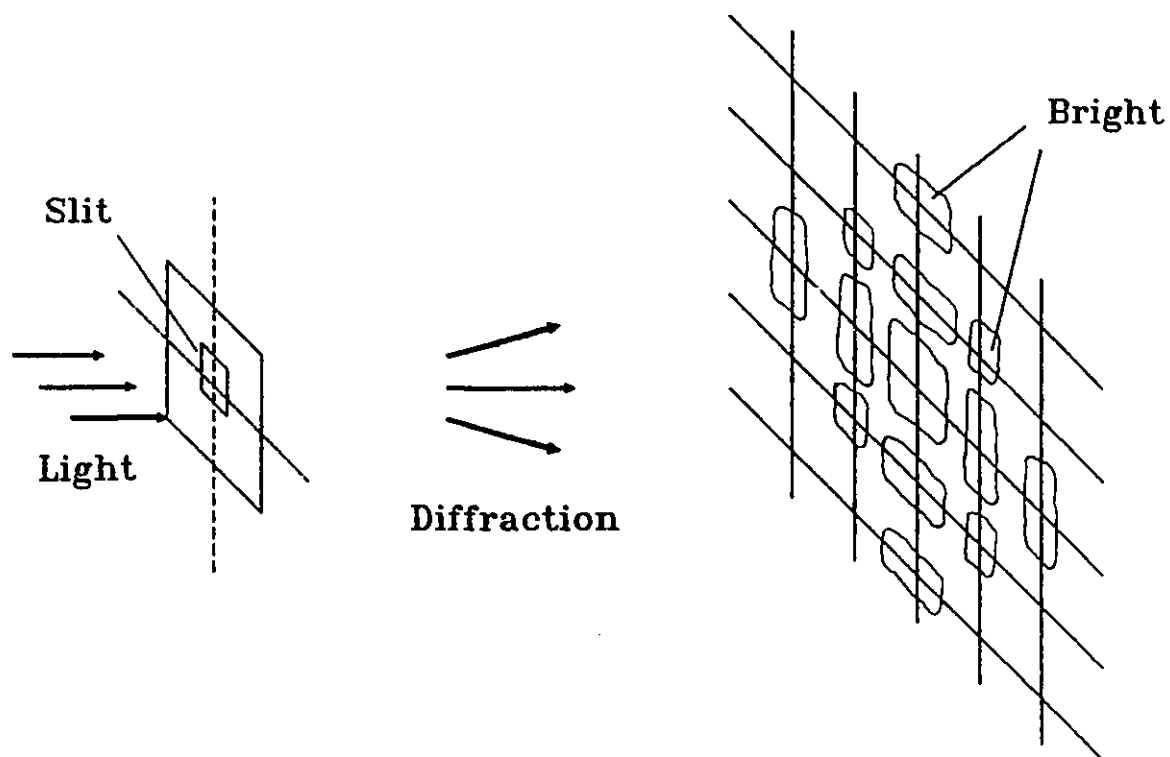
Figure 2.4b 2-D light diffraction through a square slit
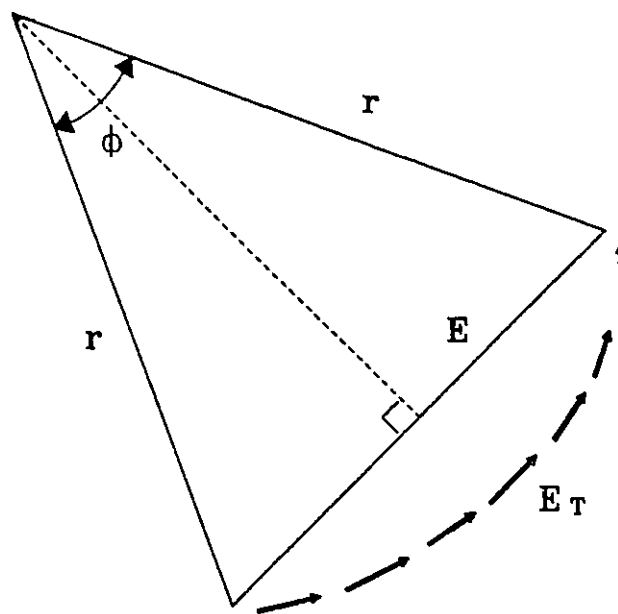
Figure 2.5 Phasor diagram for a larger number of sources
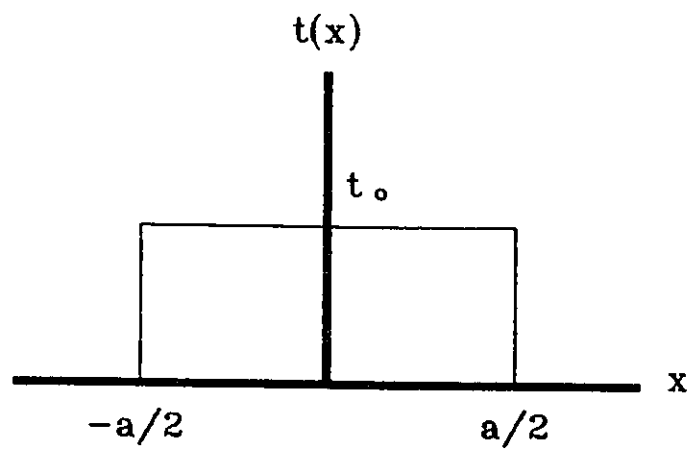
Figure 2.6 A slit function
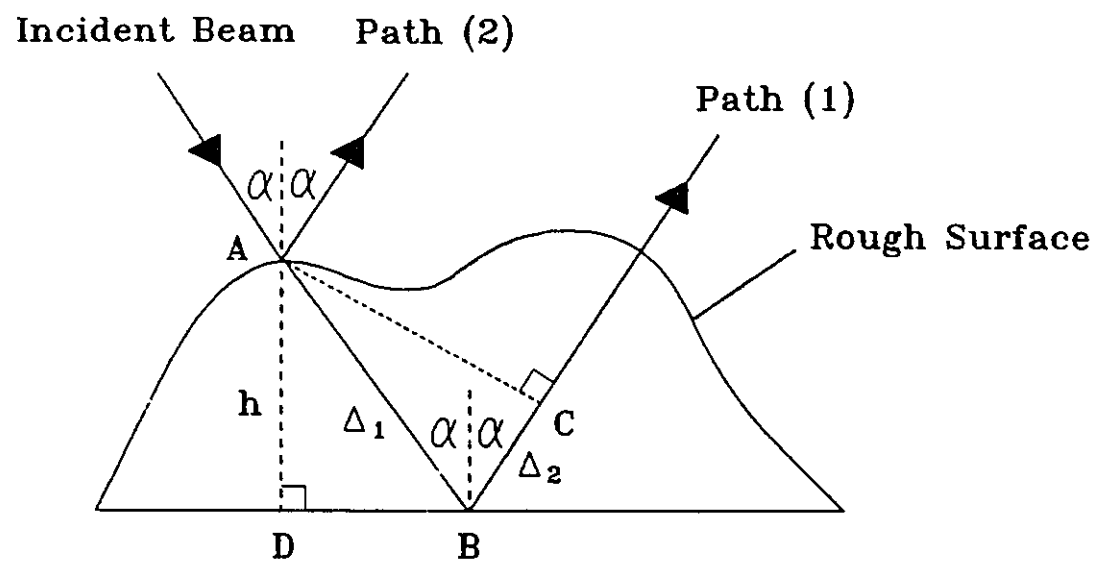
Figure 2.7 Path difference produced by surface roughness

Incident Beam

Specular
Compoment

Intensity
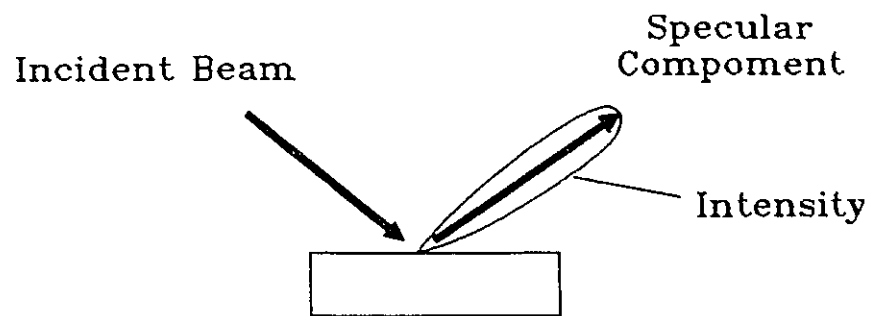
Figure 2.8a   Polar plot of light reflected from
smooth surface

Incident Beam

Specular
Compoment

Intensity
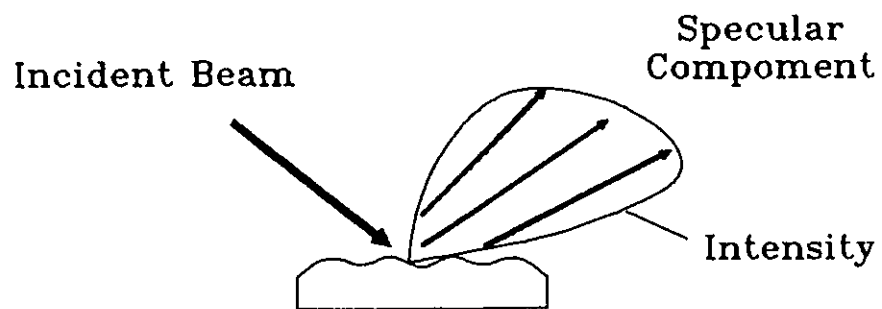
Figure 2.8b   Polar plot of light reflected from
rough surface

CHAPTER III

THEORY

When a light beam is incident on a rough surface, it will be transmitted, absorbed and scattered. The phenomenon of light scattering from a rough surface will be studied in order to develop an optical technique for surface roughness measurement. In this chapter, a brief description of light scattering geometry is given, followed by a discussion of light scattering from some surfaces. The light scattering measurement method of Bi-directional Reflective Distribution Function (BRDF) is introduced. Finally, the roughness parameters are described.

3.1 Light Scattering

When a light beam is incident on a surface, it is scattered in all directions. A diagram of light scattering geometry is shown in Figure 3.1 [Beckmann & Spizzichino, 1963]. Plane (1) is the plane of incidence and plane (2) is a plane in consideration. The angle of incidence θ_1 and the scattering angle θ_2 are measured between the normal to the surface and the appropriate beam. θ_3 is the angle of lateral scattering for lateral scattering out of the plane of incidence. Note that if it is a one-dimensional light scattering, the plane of incidence and the scattering direction are on the same plane, then θ_3 equals zero.

The scattering field is far from the surface on which the scattering pattern of the surface is formed. The phase of the scattering light is modulated by the height variations of the surface. The scattering pattern in the far field can be related to the surface

25

topography. In the next section, scattering patterns of different kinds of surfaces will be discussed.

3.2 Scattering from Surfaces

Scattering patterns of smooth, rough, periodic, random, one-dimensional and two-dimensional surfaces are illustrated in Figure 3.2. An illuminated reflective sample is located in the x,y plane, and the light is scattered onto the x_0, y_0 observation plane.

a) Perfectly Smooth Surface

A perfectly smooth surface has no fluctuation on it so that the reflected energy is concentrated on the specular beam. Therefore, a bright spot with all of the reflected energy propagated is observed on the scattering field. The light scattering from a perfectly smooth surface is a 1-D light scattering whereby the angle of incidence is equal to the scattering angle and follows the law of reflection. Figure 3.3 shows the scattering pattern of a mirror.

b) Periodic Surface

The surface discussed here is a one-dimensional periodic surface. The scattering pattern consists of light spots along the X_0-axis in the observation plane in Figure 3.2b. This alignment occurs because the lay direction of the surface is parallel to the Y-axis in the reflector plane. The spacing of the light spots is determined by the grating equation [Stover, 1990]:

$$\sin\theta_n = \sin\theta_i + n\frac{\lambda}{\Lambda} \qquad (3.1)$$

26

where θ_n = reflection angle of the order n,

θ_i = incident angle,

n = integer indicating the order,

λ = illumination wavelength

Λ = wavelength of the periodic surface.

Figure 3.4 shows different diffraction orders from a given periodic surface.

Photographs of a triangular wave surface as seen through a microscope and its corresponding scattering pattern are shown in Figures 3.5a & b.

c) One-Dimensional (1-D) Random Surface

The grinding process usually produces a 1-D surface with a given lay direction. In Figure 3.2c a 1-D random surface scatters light along the X_0-axis on the observation plane. Each wavelength on the surface produces a set of diffraction spots similar to the scattering pattern of a periodic surface. There are many wavelengths present in a random surface and these wavelengths produce different sets of diffraction spots. These spots lay along the X_0-axis on the observation plane to form the band of light (also see Figures 3.6a & b).

d) Two-Dimensional (2-D) Surface

The machining marks of the 2-D surface being discussed here extend in two directions perpendicular to each other. The scattering light of this kind of surface spreads in two directions to form two bands which cross each other as shown in Figure 3.2d. Figures 3.7a & b show the photographs of a 2-D surface (by a lapping process) through a microscope and its corresponding scattering pattern.

27

e) Isotropic Surface

Isotropic surfaces are 2-D surfaces having the same property in any direction. Light is scattered all over the observation plane in all directions as shown in Figure 3.2e. Generally, the intensity of the scattering pattern decreases when the light is scattered further away from the origin of the observation plane (see Figures 3.8a &b).

The scattering pattern is related to the surface texture which can be studied for surface texture measurement. The method of measurement of scattered light will be introduced in the next section.

3.3 Bi-directional Reflective Distribution Function (BRDF)

The distribution of the light of a scattering pattern is a function of the incident angle, wavelength and power of the incident light. In addition, this pattern is a function of other parameters such as transmittance, surface finish and the index of reflection. The Bi-directional Scatter Distributions Function (BSDF) is a common form of scatter characterization. This BSDF includes several types of scatter such as Bi-directional Reflective Distribution Function (BRDF), Bi-directional Transmissive Distribution Function (BTDF) and Bi-directional Volume Distribution Function (BVDF) [Stover, 1990].

The Bi-directional Reflective Distribution Function is a major subset of the BSDF and is commonly used for measuring scattered light. The BRDF is defined as the ratio of the scattered surface radiance to the incident surface irradiance [Nicodemus, 1977] :

$$\text{BRDF} = \frac{\text{Scattered Surface Radiance}}{\text{Incident Surface Irradiance}} \qquad (3.3)$$

The scattered surface radiance is the light flux (power) scattered through a solid angle per unit illuminated area of the surface per unit projected solid angle. The projected solid angle is the solid angle times the cosine of the scattering angle. The incident surface irradiance is the light flux incident on the surface per unit illuminated area. The geometry of BRDF is shown in Figure 3.9. In this figure, the incident beam is assumed to have a uniform cross section. P_i and P_s are the light flux (power) of the incident and scattering beam respectively. θ_i is the incident angle and θ_s is the scattering angle. ϕ_s is the angle of lateral scattering. Therefore, the direction (θ_s, ϕ_s) is the direction of the scattering beam in consideration. Now the scattered surface radiance and the incident surface irradiance can be mathematically expressed as follows:

$$Scattered\ Surface\ Radiance = \frac{dP_s}{A \cdot d\Omega_s \cdot \cos\theta_s} \qquad (3.4)$$

$$Incident\ Surface\ Irradiance = \frac{P_i}{A} \qquad (3.5)$$

where P_s = light flux of scattering beam,

P_i = light flux of incident beam,

$d\Omega_s$ = unit solid angle,

θ_s = scattering angle,

A = unit illuminated area on the surface.

Therefore, the Equation (3.3) is now:

$$BRDF = \frac{dP_s}{P_i \, d\Omega_s \cos\theta_s} = \frac{dP_s/d\Omega_s}{P_i \cos\theta_s} \qquad (3.6)$$

The Rayleigh-Rice vector perturbation theory relates the power density of the scattering light per unit incident power to the surface power spectral density function as [Rice, 1951] :

$$\frac{(dP_s/d\Omega_s) \, d\Omega_s}{P_i} = (\frac{16\,\pi^2}{\lambda^4}) \cos\theta_i \cos^2\theta_s \, Q \, S(f_x, f_y) \, d\Omega_s \qquad (3.7)$$

The left hand side of the above equation is the power scattered in the scattering direction through the unit solid angle per unit incident power. The λ on the right side of the equation is the illumination wavelength. θ_i and θ_s are the incident and scattering angles respectively. Q is a dimensionless reflectivity polarization factor which relates to the sample material properties. $S(f_x, f_y)$ is the two-dimensional surface power spectral density function of the scattering pattern in terms of the sample surface spatial frequencies f_x and f_y (see Figure 3.10). By comparing Equations (3.6) and (3.7), it can be observed that the BRDF is related to the power spectral density, $S(f_x, f_y)$, of the scattering pattern:

$$BRDF = \frac{16\,\pi^2}{\lambda^4} \cos\theta_i \cos\theta_s \, Q \, S(f_x, f_y) \qquad (3.8)$$

On the other hand, the BRDF is also related to the illumination wavelength (λ). Coherent light, such as laser, has to be used as the light source in order to provide a narrow band of illumination wavelength.

Optical surface roughness parameters derived from the power spectral density of the scattering pattern based on the Bi-directional Reflective Distribution Function will be obtained to correlate the mechanical roughness parameters. These roughness parameters will be discussed in the next section.

3.4 Roughness Parameters

The power spectral density of the scattering pattern can be found by using the Fourier analysis and the random signal theory. The Fourier transform was shown by B.J. Baptiste Fourier that any periodic wave form can be generated by adding up sine or cosine waves of different frequencies and amplitudes. A spatial domain function is transformed into a frequency domain function by the Fourier transform:

$$G(f) = \mathcal{F}[g(x)] = \int_0^x g(x)\, e^{-j2\pi fx}\, dx \qquad (3.9)$$

where G(f) = frequency domain function,

g(x) = spatial domain function,

$\mathcal{F}[\ ]$ = Fourier transform.

By performing the inverse transform, the spatial domain can be recovered:

$$g(x) = \mathcal{F}^{-1}[G(f)] = \int_0^f G(f)\, e^{j2\pi fx}\, df \qquad (3.10)$$

The distance average power, borrowed from electrical engineering terminology, is defined as:

31

$$P_{ave} = \lim_{T \to \infty} \frac{1}{T} \int_0^T g^2(x) \, dx \qquad (3.11)$$

where P_{ave} = distance average power,

T = a finite spatial distance.

The following equation is obtained by substituting Equation (3.10) into (3.11) :

$$P_{ave} = \int_0^T \lim_{T \to \infty} \frac{[G(f)]^2}{T} \, df \qquad (3.12)$$

The power spectral density, S(f), is the spatial domain function height squared per unit spatial distance. Therefore, the power spectral density of the deterministic spatial domain function is given by the integrand in Equation (3.12):

$$S(f) = \lim_{T \to \infty} \frac{[G(f)]^2}{T} \qquad (3.13)$$

Note that the G(f) term in the above equation is the amplitude of the frequency domain Fourier transform function of the spatial domain function. Thus, the power spectral density is proportional to the square of this amplitude. The zero moment (M_0) and the second moment (M_2) of the spatial domain function are defined as :

$$M_0 = \sqrt{\int (2\pi f)^0 S(f) \, df} = \sqrt{\int S(f) \, df} \qquad (3.14)$$

$$M_2 = \sqrt{\int (2\pi f)^2 S(f) \, df} = 2\pi \sqrt{\int f^2 S(f) \, df} \qquad (3.15)$$

32

In summation form, they are [Stover, 1990]:

$$M_0 = \sqrt{\sum S(f) \, \Delta f} \qquad (3.18)$$

$$M_2 = 2\pi \sqrt{\sum f^2 S(f) \, \Delta f} \qquad (3.19)$$

Surface statistics can be found by calculating the zero and the second moments of the scattering pattern of a surface. The measurable quantity of the scattering pattern of a surface is the greylevel intensity of the pattern. The intensity of a function is directly proportional to the square of the amplitude of the function [Morgan, 1953]. Therefore, the greylevel intensity of a scattering pattern is proportional to the square of the amplitude of the scattering pattern. Thus, the greylevel intensity of a scattering pattern, I(f), is proportional to the power spectral density function, S(f). The greylevel intensity can be measured and used to obtain the zero and second moments of the scattering pattern intensity of a surface:

$$M_0 = \sqrt{\sum I(f) \, \Delta f} \qquad (3.20)$$

$$M_2 = 2\pi \sqrt{\sum f^2 I(f) \, \Delta f} \qquad (3.21)$$

The above equations can be extended for a 2-D scattering pattern of a 2-D texture surface as follows:

$$M_0 = \sqrt{\sum [I(f_x, f_y) \, \Delta f_x \Delta f_y]} \qquad (3.22)$$

33

$$M_2 = 2\pi \sqrt{\sum [(f_x^2 + f_y^2) I(f_x, f_y) \Delta f_x \Delta f_y]} \qquad (3.23)$$

The f_x and f_y are the spatial frequencies as mentioned in section 3.3. These spatial frequencies can be transformed from the spatial distances of the scattering pattern via [Kurada, 1988] :

$$f_x = \frac{d_x M}{\lambda l} \qquad (3.24)$$

$$f_y = \frac{d_y M}{\lambda l} \qquad (3.25)$$

where d_x, d_y = spatial distances of the scattering pattern in x and y-directions,

M = magnification of the system,

λ = illumination wavelength,

l = focal length of the transform lens.

The optical roughness parameters, zero moment of the greylevel intensity of the scattering pattern (M_0') and second moment of the greylevel intensity of the scattering pattern (M_2') are calculated by :

$$M_0' = \sqrt{\sum I(f_x, f_y)} \qquad (3.26)$$

$$M_2' = 2\pi \sqrt{\sum f^2 I(f_x, f_y)} \qquad (3.27)$$

These optical roughness parameters are used to correlate the mechanical roughness parameters, root mean square (RMS) roughness and RMS slope of the surface profile. The

RMS roughness (σ) can be simply found via :

$$\sigma = \sqrt{\frac{1}{L} \int_0^L [z(x)]^2 dx} \qquad (3.28)$$

All notations in the above equation are referred to Equation 1.1 in section 1.1. The RMS slope (m) can be obtained from the surface profile:

$$m = \sqrt{\frac{1}{L} \int_0^L [\frac{d(z(x))}{dx}]^2 dx} \qquad (3.29)$$

or from the Fourier transform of the surface profile [Bendat & Piersol, 1971]:

$$m = \sqrt{\frac{1}{T} \int_0^f [2\pi f Z(f)]^2 df} \qquad (3.30)$$

where Z(f) = Fourier transform of the surface profile,

f = surface profile spatial frequency,

T = finite spatial distance of the profile.
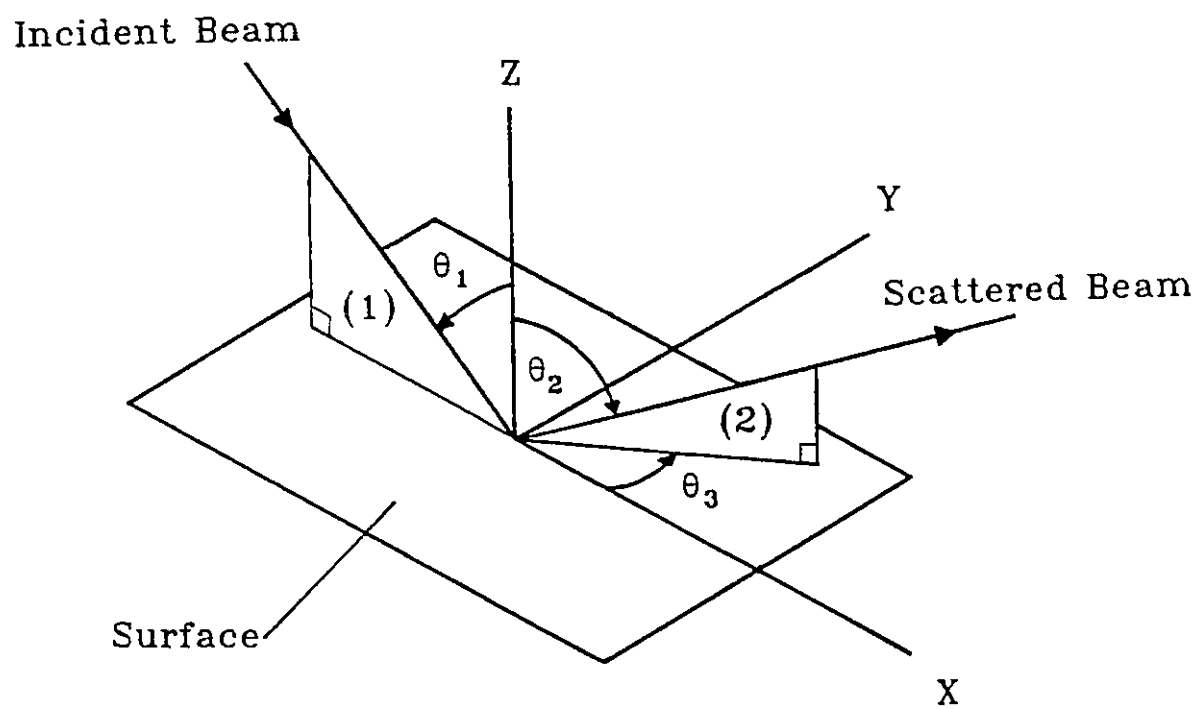
Figure 3.1 Geometry of light scattering
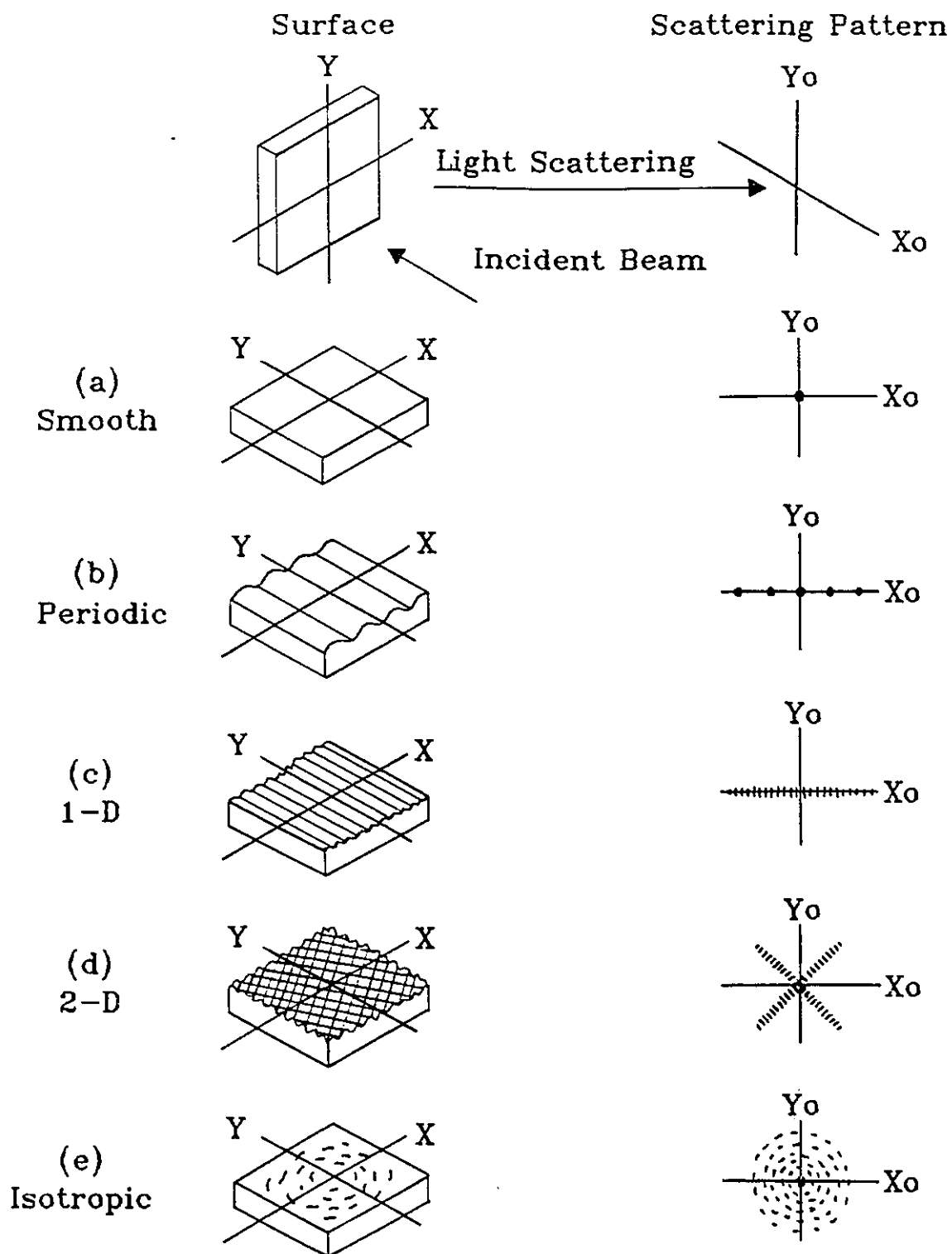
Figure 3.2 Light scattering from different surfaces
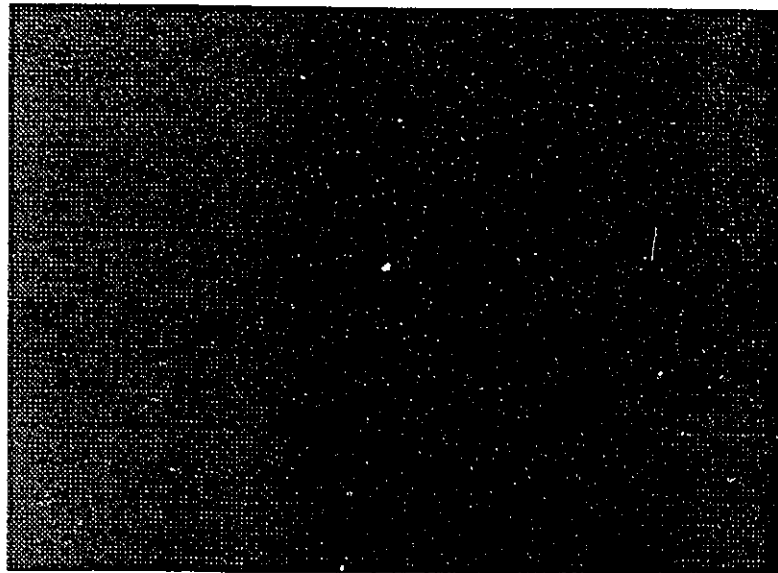
Figure 3.3   Scattering pattern of a perfectly smooth surface

Periodic Surface

Incident
Beam

θ_i

θ_{-1}

θ_o

θ_1

$n = 2$

$n = 1$

$n = 0$

$n = -2$

$n = -1$

Specular
Component

Surface Normal
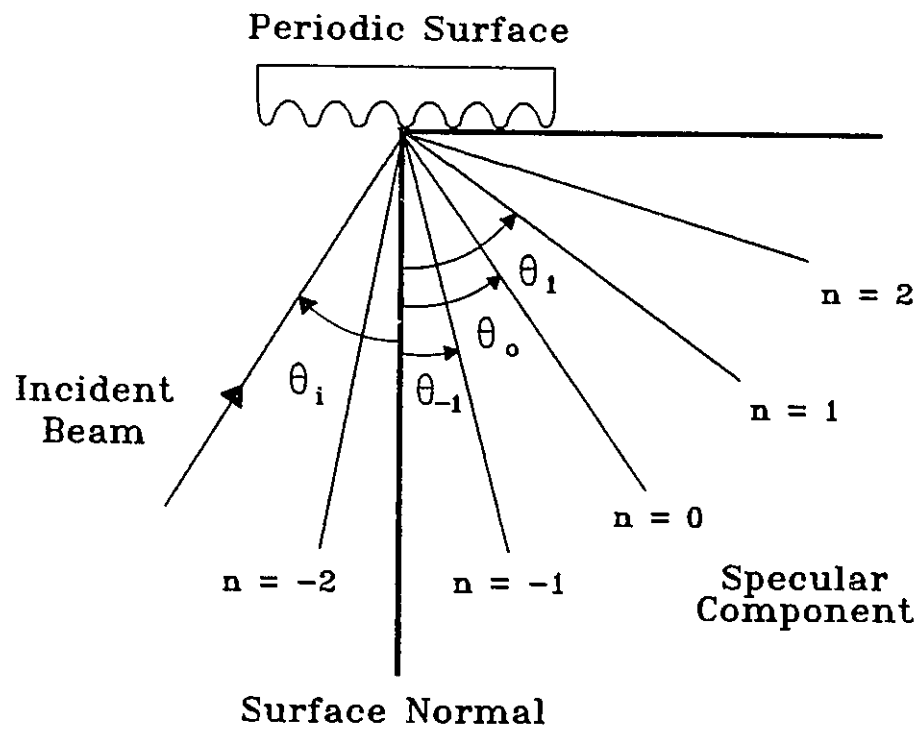
Figure 3.4 Diffraction from a periodic surface
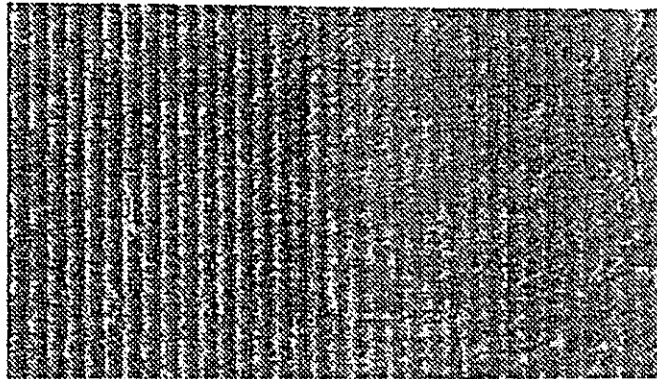
(a)
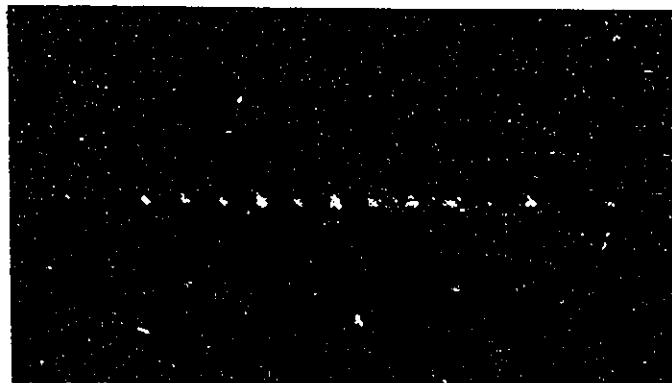
(b)

Figure 3.5 Periodic surface
a) Photograph of the surface as seen
on the microscope
b) The corresponding scattering pattern

40
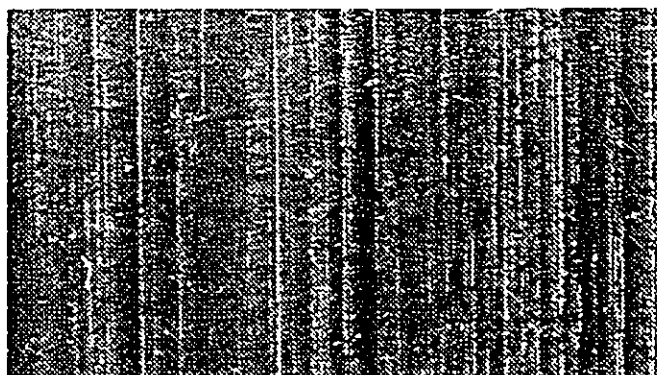
(a)
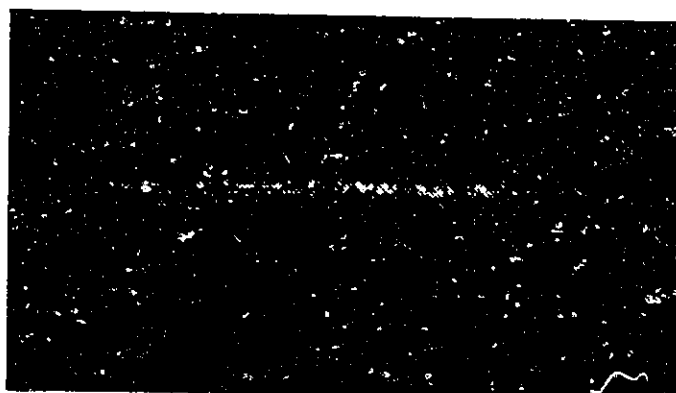
(b)

Figure 3.6 One-dimensional random surface
          a) Photograph of the surface as seen
            on the microscope
          b) The corresponding scattering pattern

41

(a)

(b)

Figure 3.7   Two-dimensional surface

    a) Photograph of the surface as seen
       on the microscope

    b) The corresponding scattering pattern

(a)
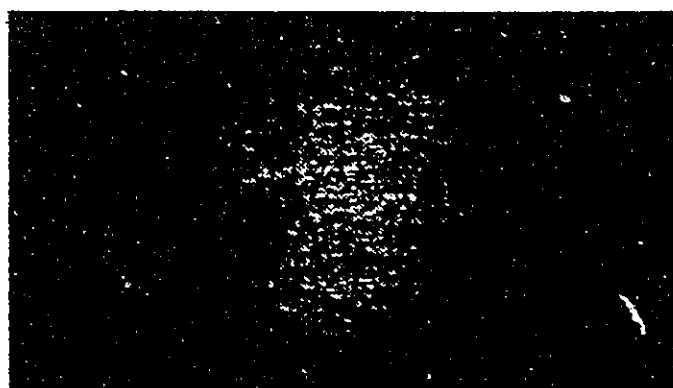
(b)

Figure 3.8 Isotropic surface
  a) Photograph of the surface as seen
     on the microscope
  b) The corresponding scattering pattern

43
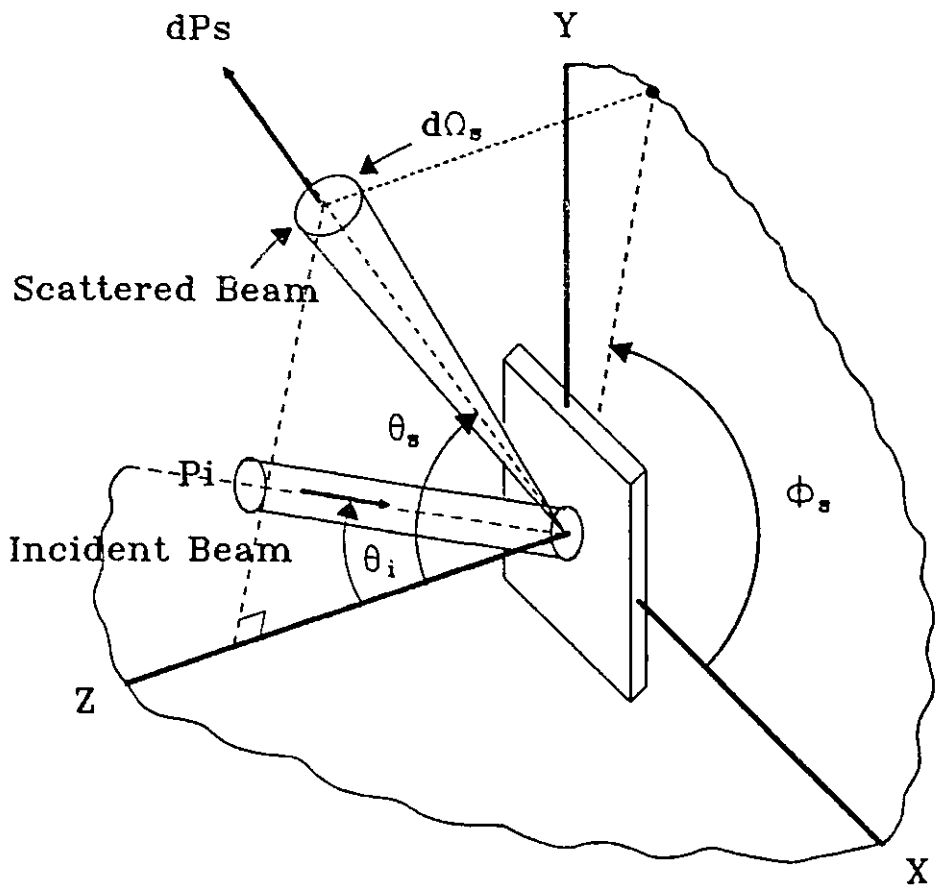
Figure 3.9 Geometry of the Bi-directional Reflective
Distribution Function (BRDF)
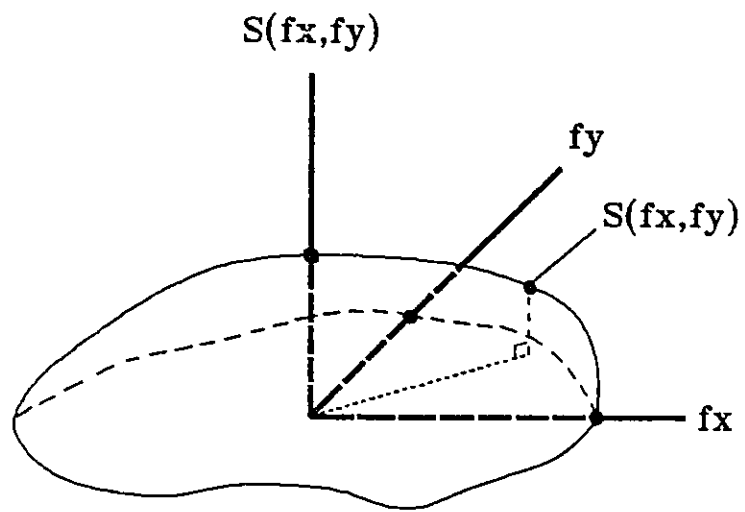
Figure 3.10 A two-dimensional power spectrum

CHAPTER IV

. APPARATUS AND PROCEDURE

The light scattering technique is used to study the surface texture of roller bearings. The greylevel intensity of the scattering pattern of a surface is used to calculate the optical roughness parameters. The apparatus and procedure used for obtaining the scattering pattern are described in this chapter. The optical roughness parameters are used to correlate the mechanical roughness parameters. Therefore, the apparatus and procedure of the mechanical measurement are also described. Finally, the description of the sample surfaces for this experiment are given.

4.1 Optical Method

4.1.1 Optical Measurement Apparatus

A schematic diagram of the optical measurement setup is shown in Figure 4.1. The specifications of the main components of the setup are in Appendix A. The light source is a 5mW He-Ne laser. The laser beam illuminates the sample surface to produce a scattering effect. The scattered pattern is magnified by an objective lens, with a magnification of 10x, onto a folding mirror. The pattern is then focused by a magnifying lens onto a CCD camera. The scattering pattern is captured by the CCD camera, then transferred to a frame grabber board and digitized to an 512x512x8bits of pixels image. The digitized image is displayed on a black and white 800x600 pixels resolution monitor. The digitized scattering pattern is now in the form of 512x512 pixels and 256 greylevels

of intensity. An IBM-PC computer is used to process the image. The zero and second

moments of the scattering pattern greylevel intensity are calculated.

4.1.2 Optical Measurement Procedure

The roller bearing samples were held by a custom made stand in order to provide

a horizontal surface for measurement. The sample was positioned at a location under the

laser beam. The laser beam was illuminated on the very top of the circumference of the

roller bearings as shown in Figures 4.2a & b. The distance between the objective lens and

the bearing surface was adjusted until a good image of the scattering pattern was

obtained. Figures 4.3a & b show an out-of-focus and a focused scattering pattern,

respectively. The zero and second moments of the bi-directional reflective distribution

function (BRDF) of the scattering pattern can then be calculated. Appendix C shows a

computer program listing for digitization and calculation process.

4.2 Mechanical Method

4.2.1 Mechanical Measurement Apparatus

A schematic diagram of the mechanical measurement setup is shown in Figure 4.4.

The stylus of a Mitutoyo Surftest III stylus instrument travels along the sample surface.

The signal from the stylus instrument is in time domain. The signal is amplified by a

signal amplifier and then transferred to a 12-bit A/D interface board in an IBM-PC

computer. The A/D interface board converts the amplified analog signal of the stylus

instrument into a digital signal. The digitized signal can then be analyzed by the

SNAPSHOT-SNAPCAL-SNAP FFT software (HEM Data Corporation) in the computer.

47

The mechanical roughness parameters can be obtained from the surface profile or the Fourier transform of the surface profile. The specifications of the main components of the mechanical measurement setup are in Appendix A.

4.2.2 Mechanical Measurement Procedure

The same custom made stand was used to hold the tapered roller bearings for the stylus measurement as shown in Figure 4.5. When a 1-D surface texture sample was measured, the direction of the stylus movement was perpendicular to the lay direction of the surface as shown in Figure 4.6a. The direction of the stylus movement for measuring a 2-D surface texture sample is shown in Figure 4.6b. The travelling speed of the stylus was set at 2 mm/s. The travelling distance was 2 mm with a 0.08 mm cutoff. The sweep time was 1 second. The sampling rate was 4000 Hz. The RMS roughness of the surface profile was obtained directly from the surface profile. The RMS slope of the surface profile was obtained from the frequency domain Fourier transform of the profile.

4.3 Sample Surfaces

A total of thirty-three sample surfaces from eleven roller bearings were tested. All roller bearings are the same size as shown in Figure 4.7 and made of the same material. The roller bearings were originally in three different categories:

1) Finished : This type of roller bearing is produced by a grinding process with a 1-D surface texture on the surface. The average RMS roughness (σ) is 0.325 µm.

2) Second pass : This type of bearing is also produced by a grinding process with a 1-D surface texture. The average RMS roughness is 0.481 µm.

48

3) Honed : This type of bearing is honed with a 2-D surface texture. The average RMS roughness is 0.174 μm.

Additional polishing was applied to all three types of the original roller bearings in order to obtain a wide range of surface roughness of 1-D and 2-D surface textures. 150- and 240- grid aluminum oxide (AlO) abrasive cloths were used to polish the roller bearings. The polishing process for generating two types of surfaces is described in the following sections.

4.3.1 Type I Polished Bearing Surfaces

A schematic diagram of an additional polished bearing sample contains a composite 1-D and 2-D surface texture for the experiment as shown in Figure 4.8a. There are three regions of texture on the bearing: two 1-D texture regions and one 2-D texture region. The procedure for obtaining this kind of sample is as follows:

1) Region A of the original roller bearing was covered by masking tape as shown in Figure 4.9a.

2) The bearing was clamped to a chuck of a lathe as shown in Figure 4.9b. It was turned on the lathe to rotate the specimen at 200 rpm in the direction shown by the arrow.

3) The bearing was manually polished by an abrasive cloth in the direction shown in Figure 4.9c. Five passes were used in order to create the first set of textures on the bearing. Since Region A was protected by masking tape, there was no additional polished texture on this region as shown in Figure 4.9d.

4) The masking tape at region A was removed and region B was covered by another

49

piece of masking tape as shown in Figure 4.9e.

5) The bearing was clamped to the chuck as shown in Figure 4.9f and rotated in the same direction with the same speed.

6) The bearing was polished using the same abrasive cloth as in region A in the direction shown in Figure 4.9g. Five passes were used to create a uniform surface texture.

7) The masking tape was removed from Region B. The bearing contained two 1-D texture sample surfaces and one 2-D texture sample surface. These regions are named as Region A, Region B & Region C as shown in Figure 4.9h.

In the hand polishing process, the abrasive cloth was held firmly in two hands and pressed onto the bearing surface. The pressure applied onto the bearing surface and the traveling speed of the abrasive cloth were kept constant during the polishing. Care was taken to ensure texture uniformity; however, scratches may have occurred to some parts of the surfaces. Therefore, the sample surface has to be examined in order to make sure the spot was uniform.

4.3.2 Type II Polished Bearing Surfaces

Another type of polished roller bearing surface has only a 2-D texture on the bearing surface as shown in Figure 4.8b. The procedure for polishing is as follows:

1) The bearing was clamped to the chuck as shown in Figure 4.10a. The bearing was rotated in the direction as shown at a speed of 200 rpm.

2) The bearing was polished by an abrasive cloth passed back and forth ten times in the direction shown in Figure 4.10b (i.e. five times backward and five times

forward).

3) The bearing had a 2-D texture all over the surface. Each bearing was divided into three regions as shown in Figure 4.10c. Each surface region was used as a particular sample of the given roughness for the experiment.

A tool was also used to hold the abrasive cloth for polishing this type of bearing in order to maintain a uniformity on the polished bearing surface. Due to the set-up error, however, the tool did not travel perfectly parallel to the bearing surface. This produced different roughnesses along the axis of the polished bearing surface. For measurement, each bearing surface was divided into three regions of different roughness as shown in Figure 4.10c.

There were six roller bearings of type I surfaces and five roller bearings of type II surfaces which gave a total of twelve 1-D texture sample surfaces and twenty-one 2-D texture sample surfaces for testing. The details of each sample surface are shown in Table 4.1 and 4.2. These samples were measured and the results will discussed in the next chapter.

Table 4.1   Details of the 1-D texture sample surfaces

Sample Surfaces	Original Type	Abrasive Cloth	Region on Bearing
A1	Finished	240	A
B1	Finished	240	B
A2	Finished	150	A
B2	Finished	150	B
A3	2nd Pass	240	A
B3	2nd Pass	240	B
A4	2nd Pass	150	A
B4	2nd Pass	150	B
A5	Honed	240	A
B5	Honed	240	B
A6	Honed	150	A
B6	Honed	150	B

Table 4.2 Details of the 2-D texture sample surfaces

Sample Surfaces	Original Type	Abrasive Cloth	Region on Bearing
C1	Finished	240	C
D1	Finished	240	D
E1	Finished	240	E
F1	Finished	240	F
C2	Finished	150	C
D2	Finished	150	D
E2	Finished	150	E
F2	Finished	150	F
C3	2nd Pass	240	C
D3	2nd Pass	240	D
E3	2nd Pass	240	E
F3	2nd Pass	240	F
C4	2nd Pass	150	C
D4	2nd Pass	150	D
E4	2nd Pass	150	E
F4	2nd Pass	150	F
C5	Honed	240	C
D5	Honed	240	D
E5	Honed	240	E
F5	Honed	240	F
C6	Honed	150	C

Magnifying
Lens

CCD Camera

Mirror

IBM−PC

Monitor

Aperture

Beam
Splitter

He−Ne Laser

Objective
Lens

Incident Beam

Reflected Beam

Sample
Surface

Signal
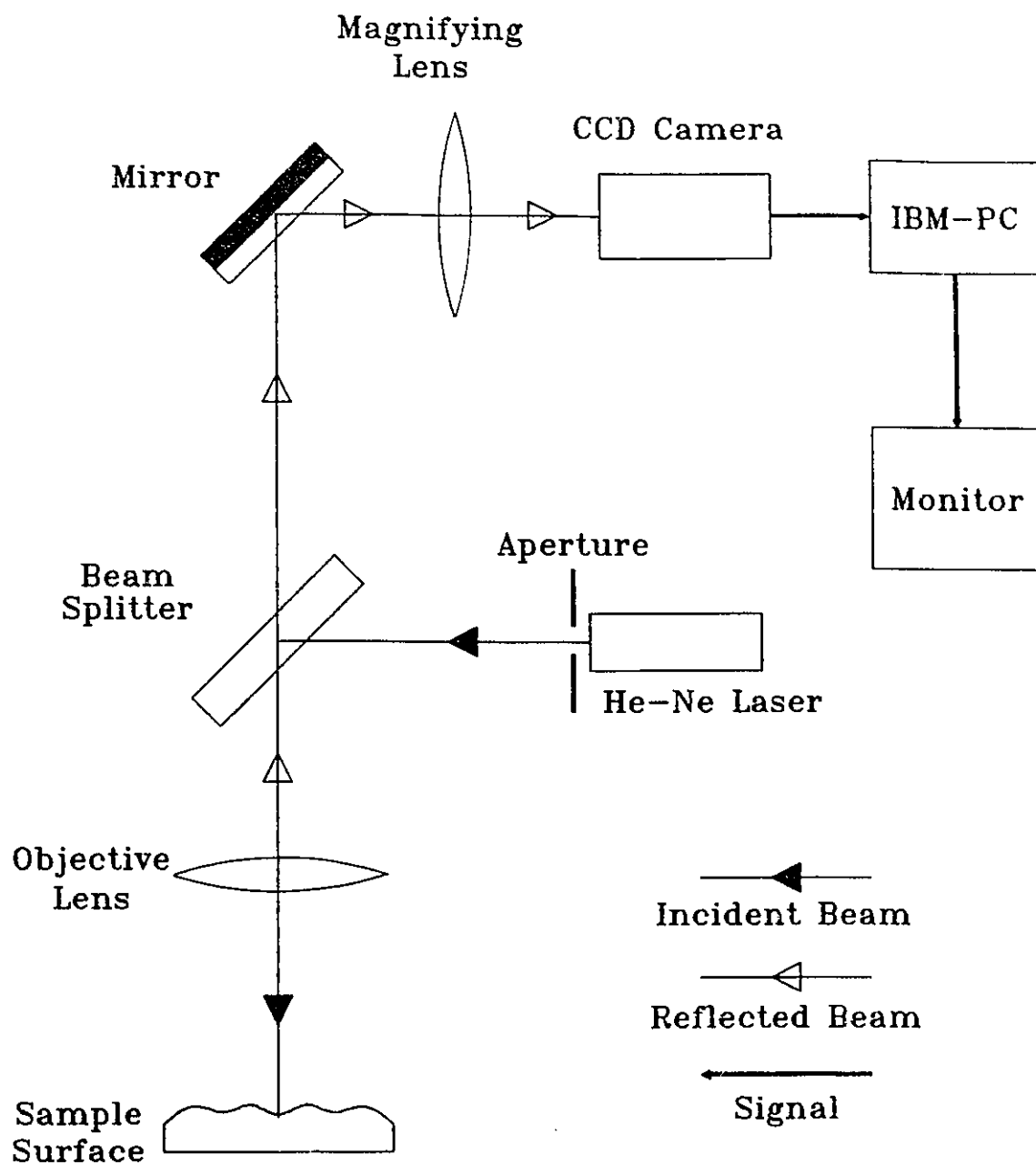
Figure 4.1   Schematic diagram of the setup for roughness
measurement using laser light scattering

Laser Beam

(a)

Roller Bearing

Custom made stand

Laser Beam

Roller Bearing

(b)

Custom made stand
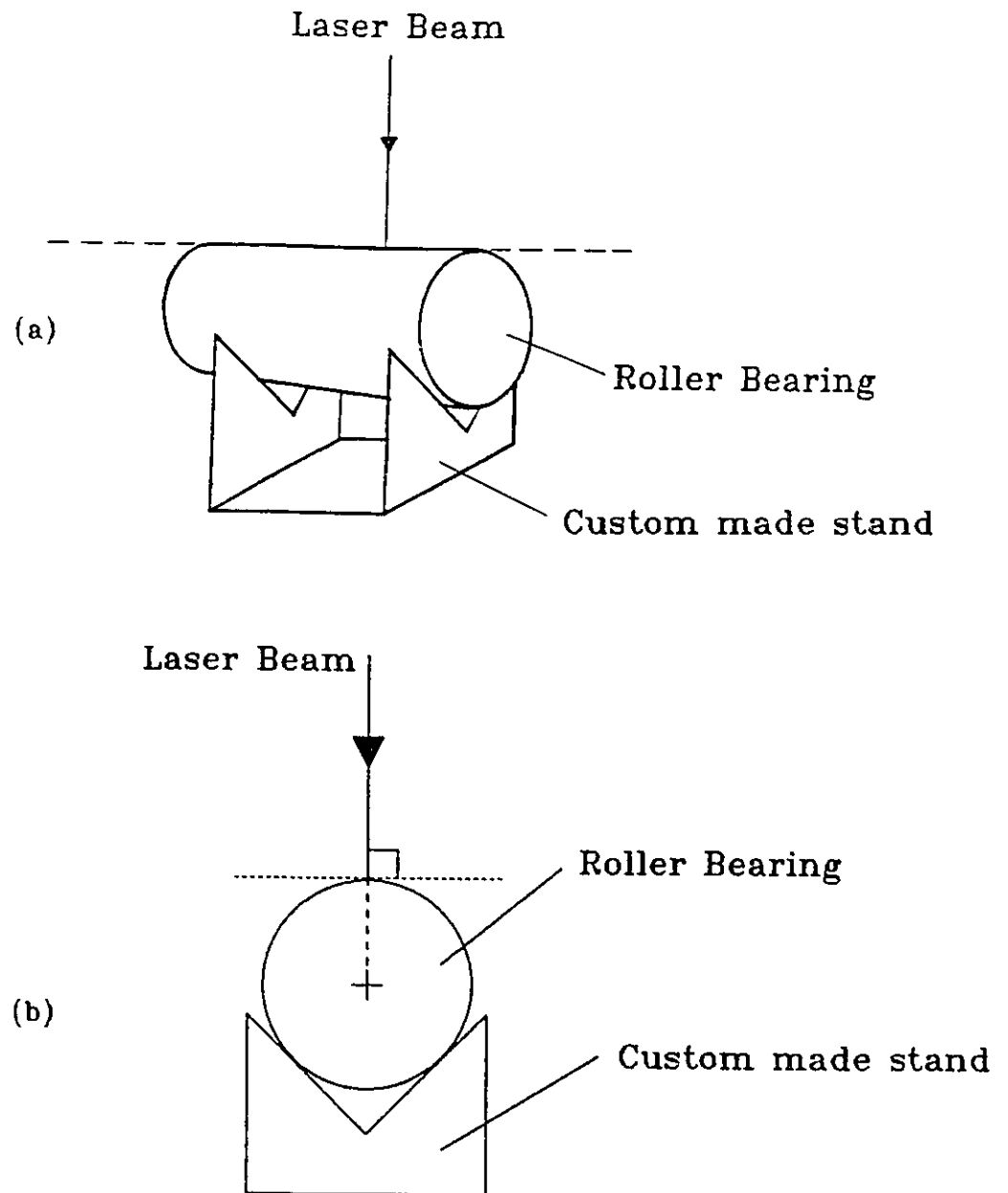
Figure 4.2   Schematic diagram of laser beam incident
            on a roller bearing
            a) Persepctive view   b) End view
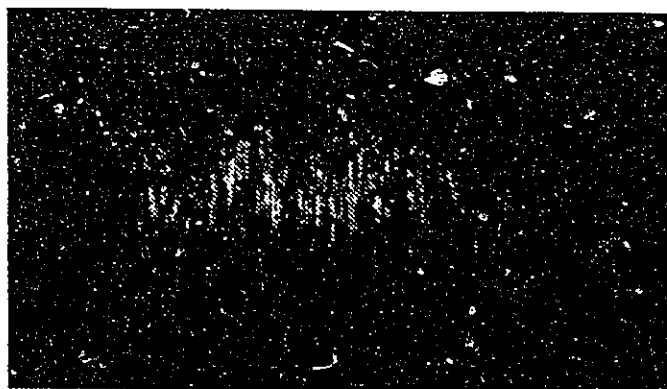
(a)
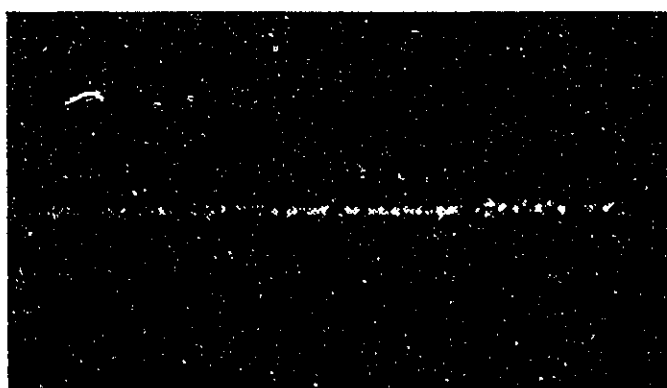
(b)

Figure 4.3 a) Photograph of an out–of–focus scattering
pattern

b) Photograph of a focused scattering pattern

56

Stylus Instrument
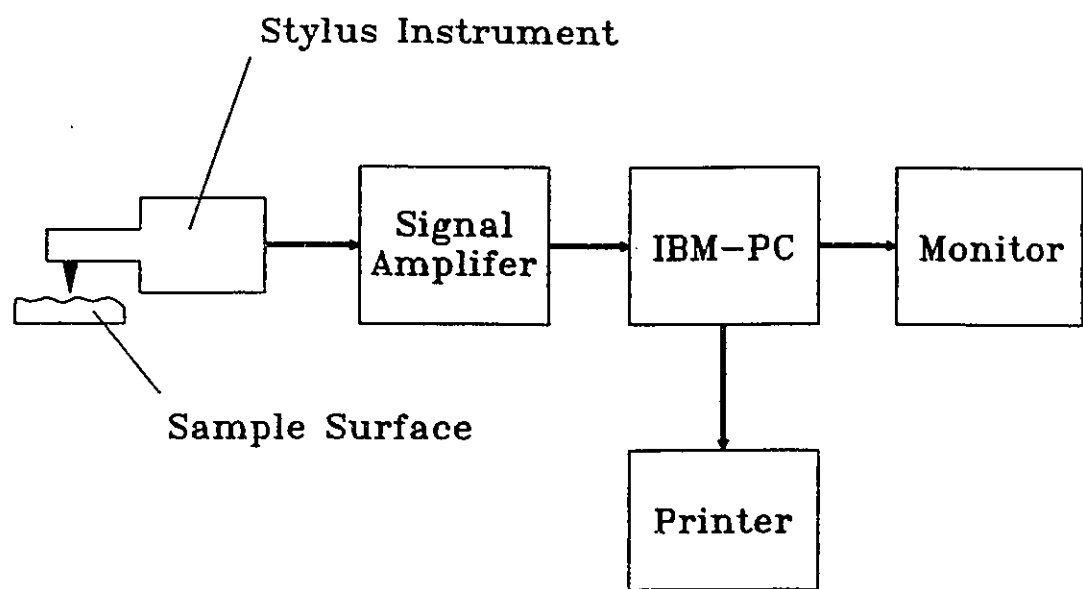
Figure 4.4 Schematic diagram of the setup for roughness
measurement using the mechanical method

(a)

Tapered Roller Bearing

Custom made stand

(b)

Tapered Roller Bearing

Stylus
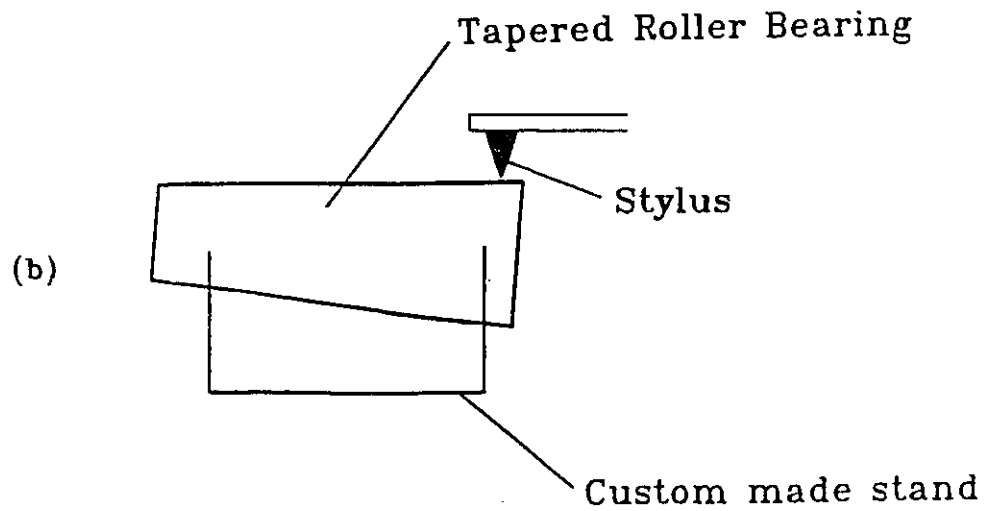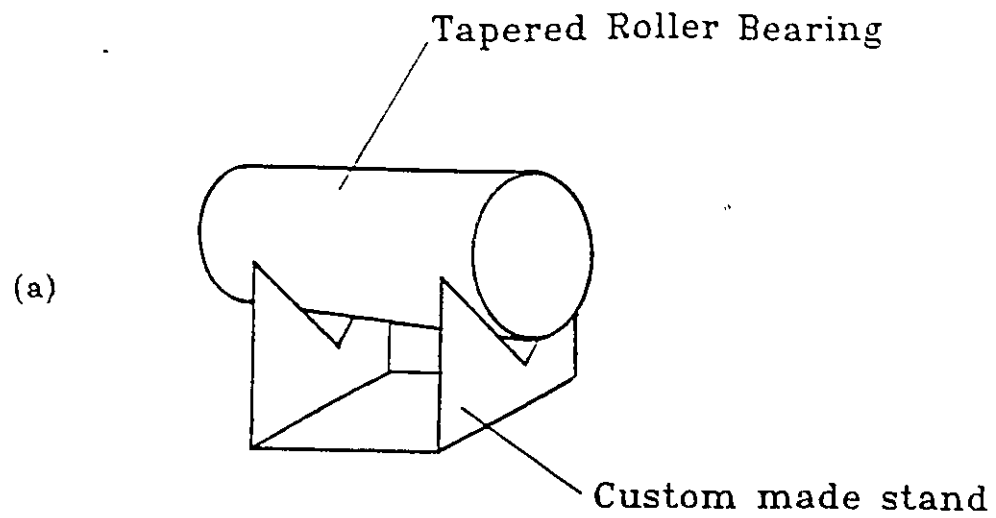
Custom made stand

Figure 4.5   Tapered roller bearing held by the custom
made stand to provide a horizontal surface
a) Perspective view   b) Side view

Lay Direction

Surface

Direction of
Stylus Movement
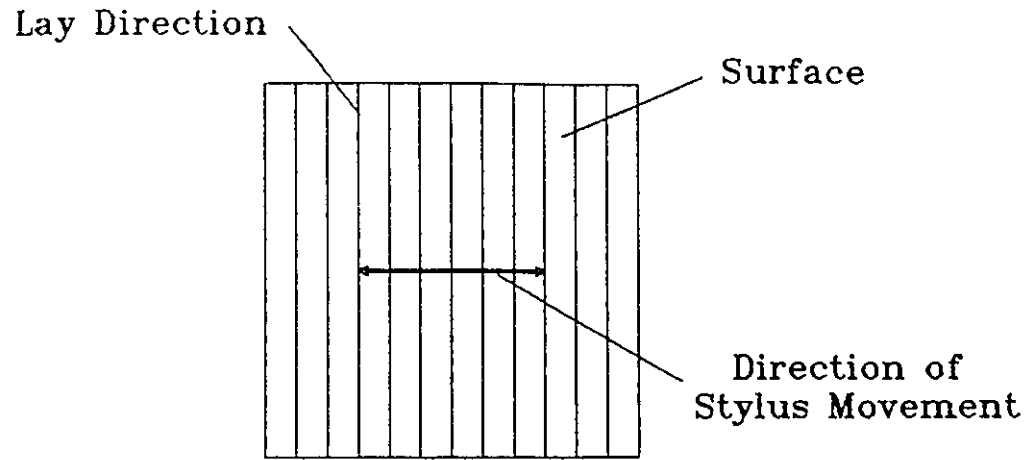
Figure 4.6a   Direction of the stylus movement for
measuring 1-D surface

Lay Directions

Surface

Direction of
Stylus Movement
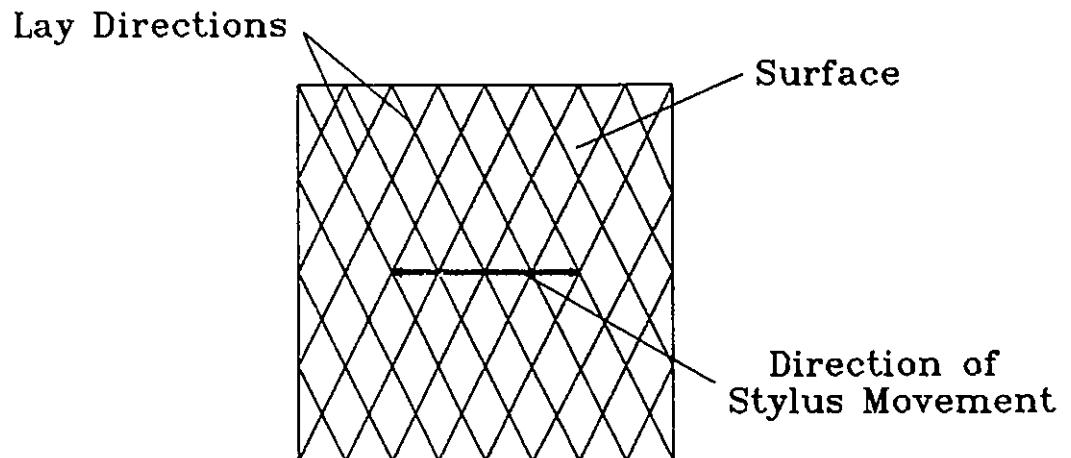
Figure 4.6b   Direction of the stylus movement for
measuring 2-D surface
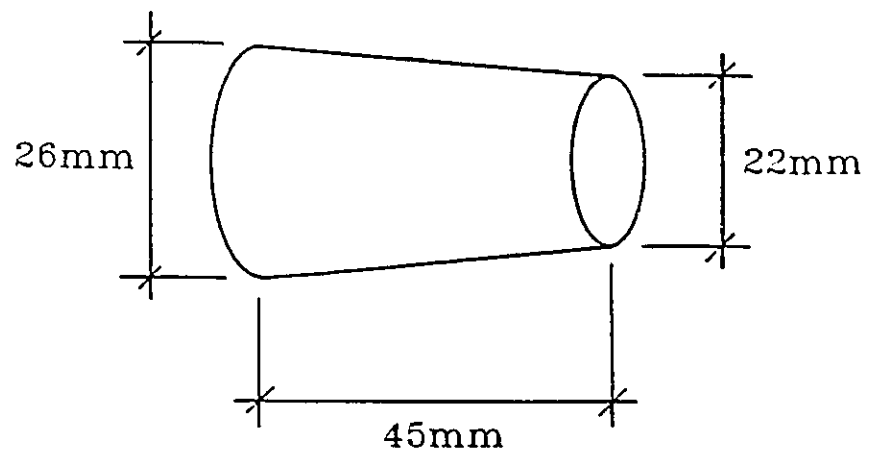
Figure 4.7 Dimensions of a Roller Bearing

1—D Texture Region

2—D Texture Region
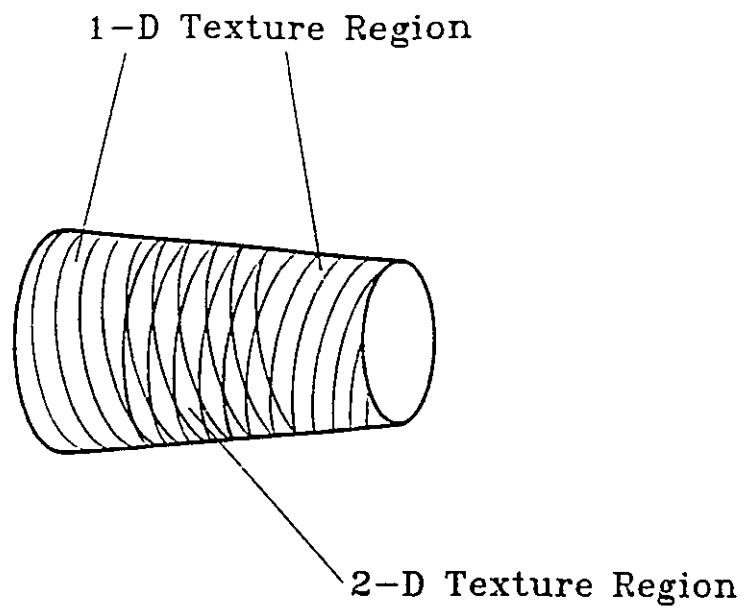
Figure 4.8a   Schematic diagram of a type I bearing surface
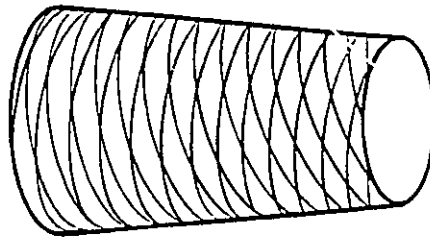
Figure 4.8b   Schematic diagram of a type II bearing surface

Original Bearing

(a)

Region A : Masking Tape

(e)

Region B : Masking Tape

(b)

(f)

(c)

(g)

Region A : No additional
polished texture

(d)

Region A   Region B

(h)

Region C
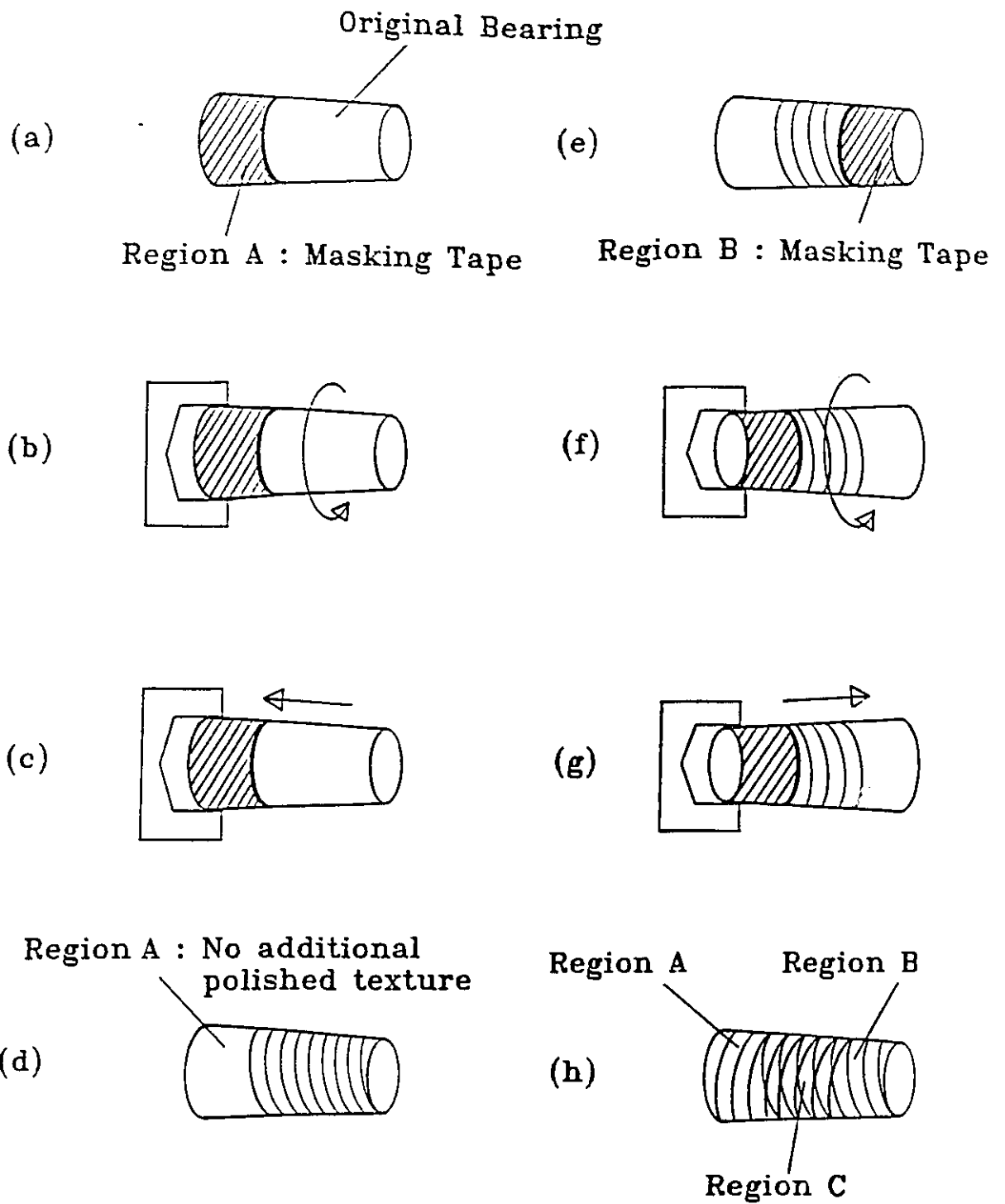
Figure 4.9a−h Procedure for creating type I bearing surface

(a)

Original Bearing

(b)

(c)

Region : D   E   F
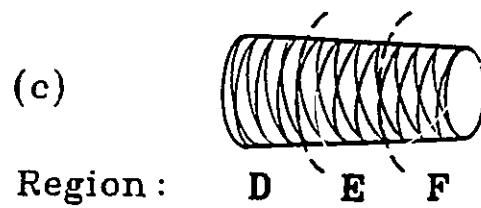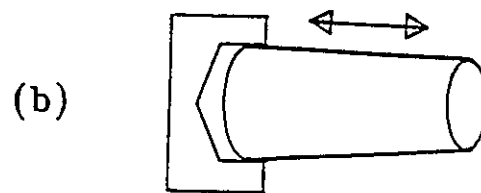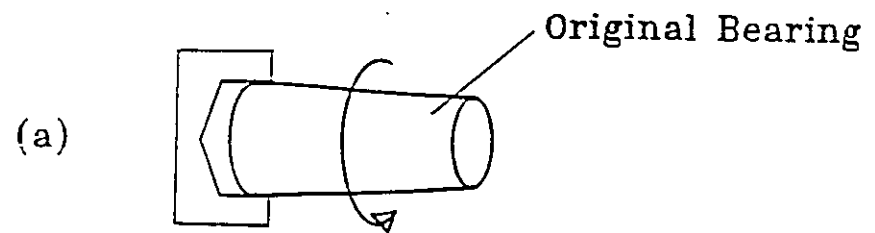
Figure 4.10a-c Procedure for creating type II bearing surface

CHAPTER V

RESULTS AND DISCUSSION

Optical zero and second moments of the bi-directional reflective distribution function (BRDF) were obtained from the scattering pattern. These were selected as optical parameters for the correlation with the surface texture parameters obtained from stylus instruments. This correlation will be discussed in this section. In order to understand the light scattered from the sample surfaces for the experiment, a description of the scattering pattern will be given first.

5.1 Scattering Patterns of the Sample Surfaces

Photographs of the typical 1-D texture surfaces of Regions A & B on a sample bearing and the corresponding scattering patterns are shown in Figures 5.1a & b and 5.2a & b respectively. The scattering patterns are similar to the scattering pattern of the 1-D surface described in section 3.2 (also see Figure 3.3). The scattering patterns are straight bands which form an angle with respect to the X_0-axis in the scattering plane. This angle is equal to the angle between the lay direction and the Y-axis in the sample surface.

Photographs of the typical 2-D texture surface on a sample bearing and the corresponding scattering patterns are shown in Figures 5.3a & b. The scattering pattern has two straight bands which cross each other. The angle between two bands is equal to the angle between the two lay directions on the surface.

5.2 Correlation Curves for 1-D Texture Surfaces

Twelve surfaces from the type I polished roller bearing surfaces containing 1-D surface texture were used in the test and their correlation curves between optical and mechanical parameters were plotted.

a) Zero Moment vs RMS Roughness

Figure 5.4 shows the correlation between optical zero moment versus mechanical RMS roughness of 1-D texture surfaces for three different laser spot intensities. For the high intensity, the measurements were made with the aperture adjusted so that the maximum intensity in the image was just below saturation. For the low intensity set-up, adjustment was made until the faintest feature of the image was detectable. For the mid intensity, the setting is somewhere between these two limits. It can be observed that the three curves are parallel to each other and have a similar trend. When roughness is small, the value of the zero moment is high and this value decreases as RMS roughness increases. The curves become flat when the RMS roughness is greater than 0.5 μm. In this region, the sensitivity of the correlation curves for 1-D surface texture bearings decreases.

A normalization of the three correlation curves was carried out in order to obtain a non-dimensional correlation curve. In this process, the sample surface A1 (RMS roughness = 0.382μm) was selected as a reference standard and the measured parameters were defined relative to the standard. The normalized data were plotted in Figure 5.5. It can be observed that one curve can be used to fit all three sets of data. It should be noted that there is a large spread of data points in the large roughness range. This is due to the low intensity of the illuminating spot which reduces the sensitivity of the CCD sensor.

On the other hand, only a few lines of the polishing marks are involved within the illumination spot in the large roughness range. Therefore, the scattering pattern may not represent the true characteristic of the surface.

b) Second Moment vs RMS Slope

The second moment was plotted against the RMS slope as shown in Figure 5.6. It can be observed that the three curves for three intensities are parallel to each other and have a similar trend. The same normalized process was carried out for these data using the same standard sample surface. The normalized curve was obtained as shown in Figure 5.7.

5.3 Correlation Curves for 2-D Texture Surfaces

Twenty-one 2-D texture surfaces of different roughness from roller bearings were used in the measurement. The relationship between optical parameters and mechanical parameters for these surfaces will be established.

a) Zero Moment vs RMS Roughness

The correlation curves for the three different laser intensities was plotted as Figure 5.8. It can be observed that these curves have a similar trend to that of 1-D texture surfaces. The curves are parallel to each other and the sensitivity of the curves becomes low when the RMS roughness is greater than 0.5μm. The sample surface C1 (RMS roughness = 0.398μm) was selected as a standard for normalizing the correlation curves. The results are shown in Figure 5.9. It can be observed that one curve can be used to fit

all three sets of data, each set associated with a given illumination intensity. It can be noted here that the spread is much less than that in the 1-D case (Figure 5.5). In addition, the fitted curve of the 2-D texture surfaces coincides with the 1-D texture surface correlation curve (Figure 5.10). Thus, this curve can be used as the correlation curve of zero moment vs RMS roughness for both 1-D and 2-D texture surfaces.

b) Second Moment vs RMS slope

Figure 5.11 shows the correlation between the RMS slope and the second moment of the 2-D texture surfaces. The correlation curves of different laser intensities show the same trend as observed previously. The same normalized process was carried out using the same 2-D standard sample surface, C1. This curve was plotted in Figure 5.12. It should be noted that there is a large spread in the data. This may be caused by the number of different calculation steps used. The RMS slope was obtained from the Fourier transform of the surface profile. The error may be large because of the transformation of the surface profile. The second moment was obtained by multiplying the square of the spatial frequencies by the greylevel intensity of the scattering. There were some errors in the conversion of the spatial frequencies.

By comparing Figure 5.7 to Figure 5.12, the fitted curve for the 2-D texture surface almost coincides with the 1-D texture surface correlation curve. These curves were plotted in Figure 5.13.

5.4 Measurement Uncertainty

The uncertainty of this optical measurement technique is determined by different

67

factors, such as: focusing the image of the pattern, centering the sample surface, and non-uniformity of the texture. This uncertainty is arbitrarily expressed by the relative error which is defined by the ratio of standard deviation and the arithmetic mean (X_m):

$$Error = \frac{Standard\ Deviation}{Mean} \times 100\%$$

$$= \frac{\sqrt{\frac{1}{k-1} \sum_{i=1}^{k} (X_i - X_m)^2}}{X_m} \times 100\% \qquad (5.1)$$

The sample surface C1 was arbitrarily selected as a standard surface for determining the measurement uncertainty.

a) Focusing Error

The sample surface was measured using the same measurement procedure as described in section 4.1.2. The zero and second moments of the scattering pattern were obtained. The sample was refocused and another measurement was made. This procedure was repeated five times and the uncertainties for both the zero and second moments were calculated. These are 2.6% & 1.9%, respectively, as shown in Table 5.1.

b) Centering Error

To check the effect of the slope (due to the curved surface) on the reflected beam, the laser spot was moved 1 mm away from the top point of the surface curvature. A measurement was made with this setting. This measurement was compared to that of the

68

beam at the top of the curvature in order to determine the centering error. The values for the zero and second moments are 5.1% & 7.5% as shown in Table 5.1.

c) Sample Non-uniformity

Due to the non-uniformity of the sample surfaces, a variation in the measurement exists when one makes measurements across the surface. Efforts were made to use the same spot for both mechanical and optical measurements. To determine whether the locating process is repeatable, the sample spot was marked and then re-located for the measurement. The sample was then moved and repositioned again for a subsequent measurement of the same spot. The difference between the two measurements was 4.8% for the zero moment and 4.4% for the second moment.

Table 5.1   Possible error in optical measurement

Error Factor	Zero Moment	Second Moment
Focusing	2.6%	1.9%
Centering	5.1%	7.5%
Non-uniformity	4.8%	4.4%

It should be noted that the error is determined based on the measurement of the sample surface C1. The error will be much higher for rougher surfaces.

69
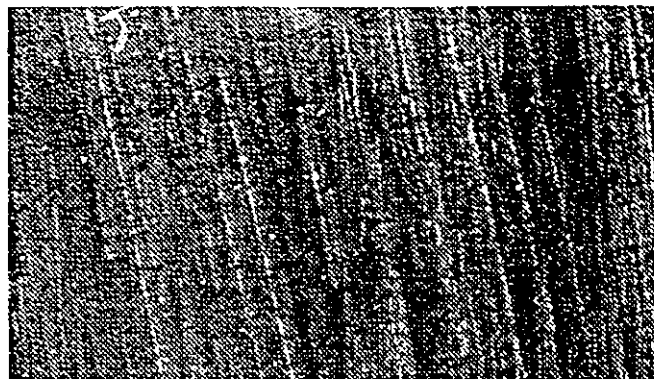
(a)
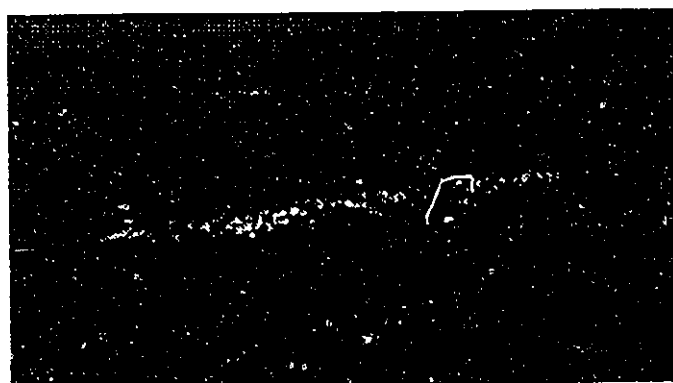
(b)

Figure 5.1   A typical 1−D sample surface (Region A)
a) Photograph of the surface as seen
on the microscope
b) The corresponding scattering pattern

70
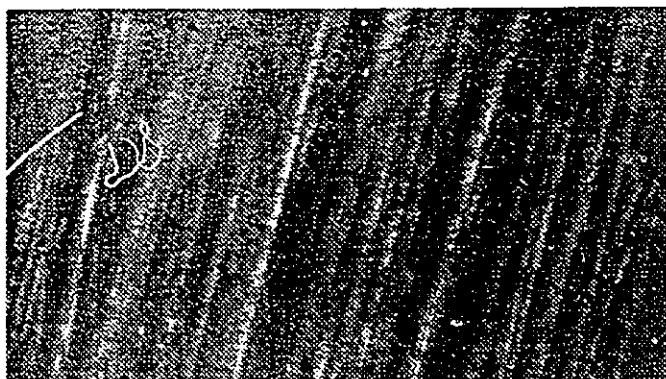
(a)

(b)

Figure 5.2 A typical 1-D sample surface (Region B)
a) Photograph of the surface as seen
   on the microscope
b) The corresponding scattering pattern

71
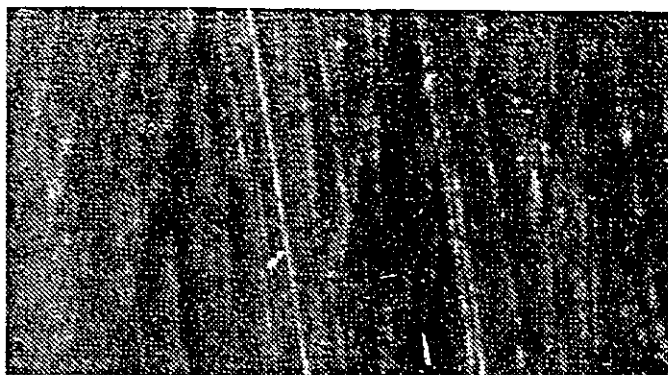
(a)

(b)

Figure 5.3 A typical 2–D sample surface
            a) Photograph of the surface as seen
               on the microscope
            b) The corresponding scattering pattern

Zero Moment vs RMS Roughness
1-D Texture Surfaces on Roller Bearings
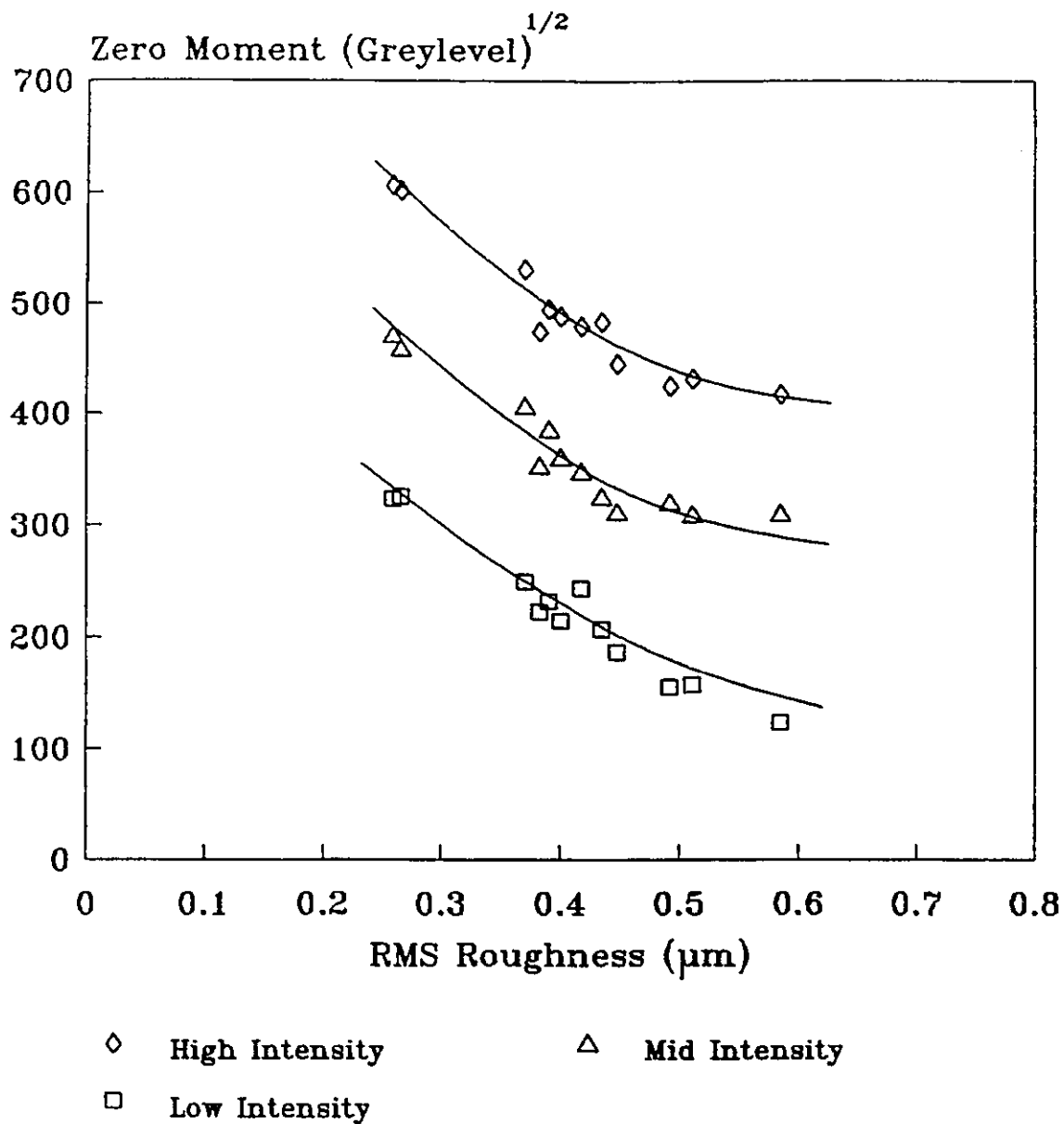
Figure 5.4 Correlation curves of
RMS roughness for 1-D texture
surfaces on roller bearings

Normalized Zero Moment vs RMS Roughness
1-D Texture Surfaces on Roller Bearings
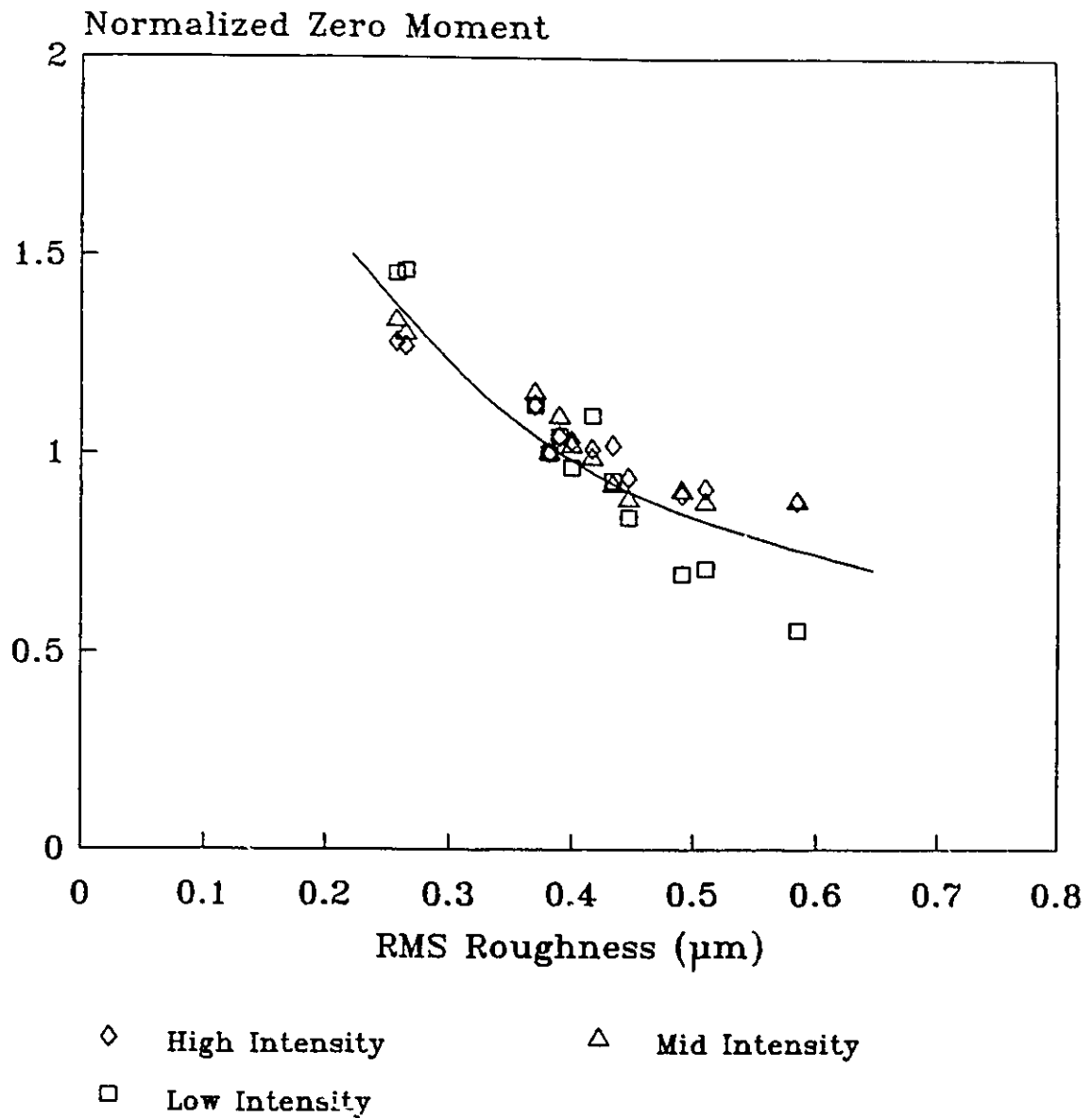
Figure 5.5 Normalized correlation curve
of RMS roughness for 1-D texture
surfaces on roller bearings

Second Moment vs RMS Slope
1-D Texture Surfaces on Roller Bearings
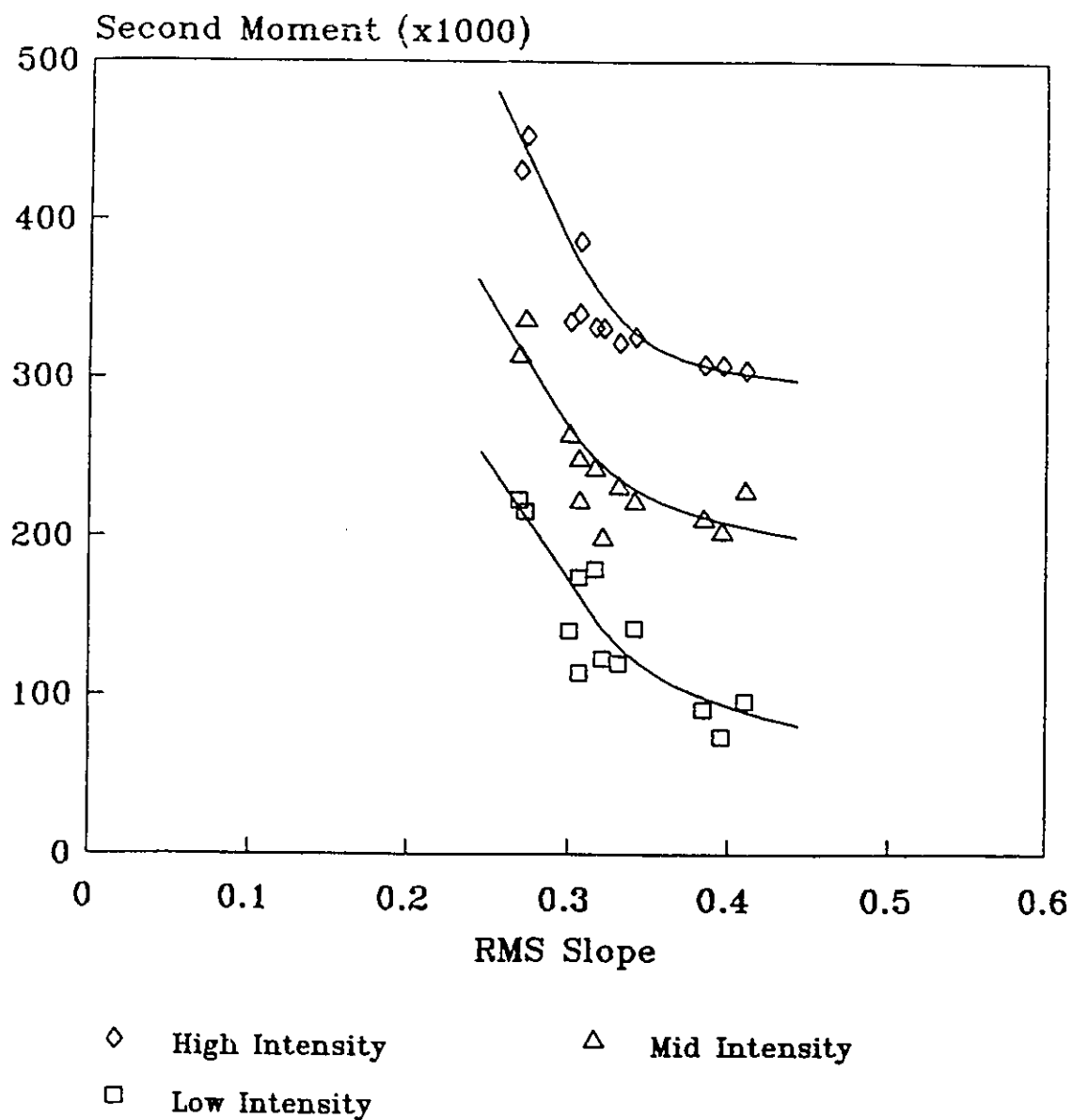
Figure 5.6 Correlation curves of
RMS slope for 1–D texture
surfaces on roller bearings

Normalized Second Moment vs RMS Slope
1−D Texture Surfaces on Roller Bearings
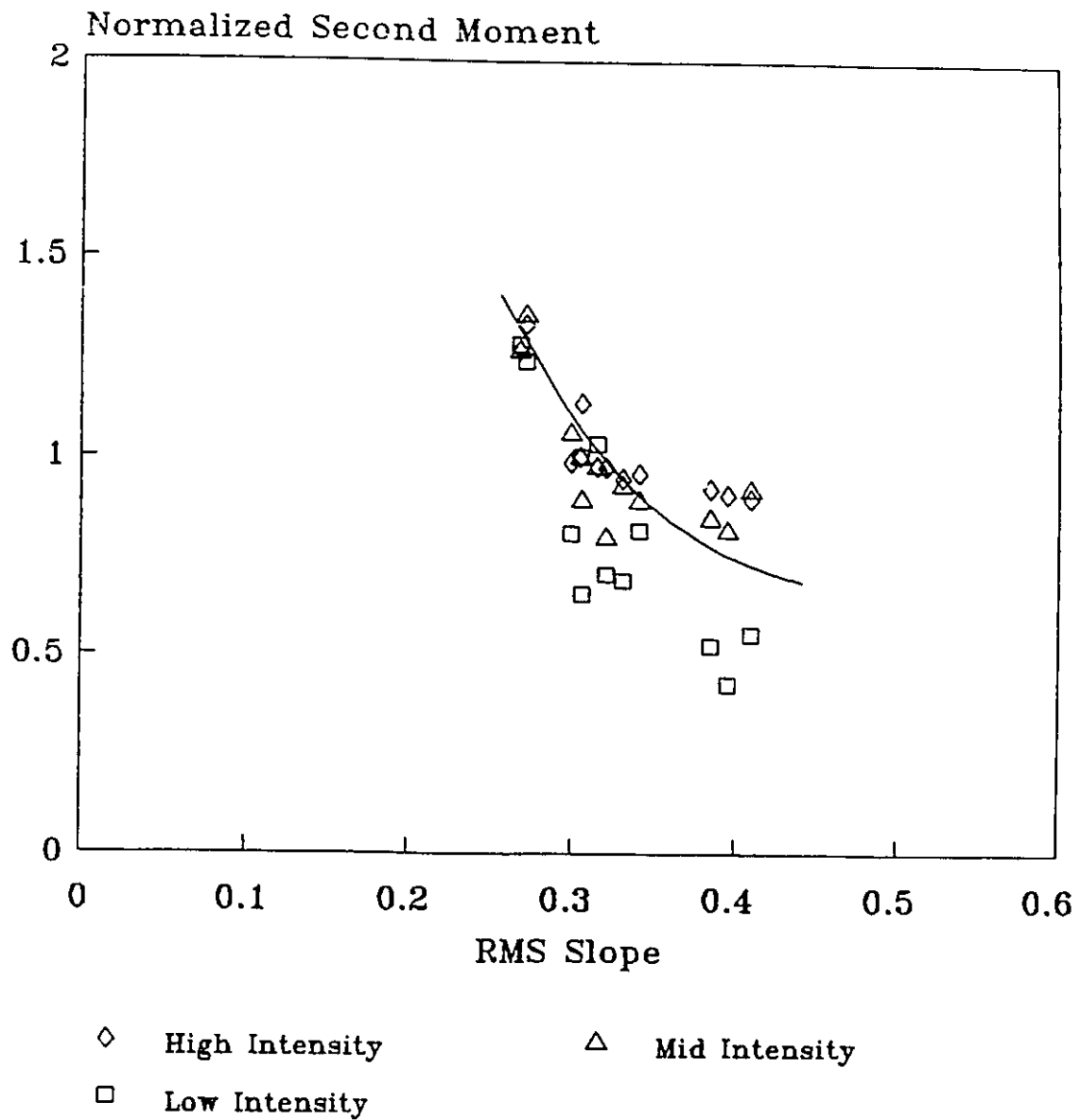
Figure 5.7 Normalized correlation curve
of RMS slope for 1−D texture
surfaces on roller bearings

76

Zero Moment vs RMS Roughness
2-D Texture Surfaces on Roller Bearings
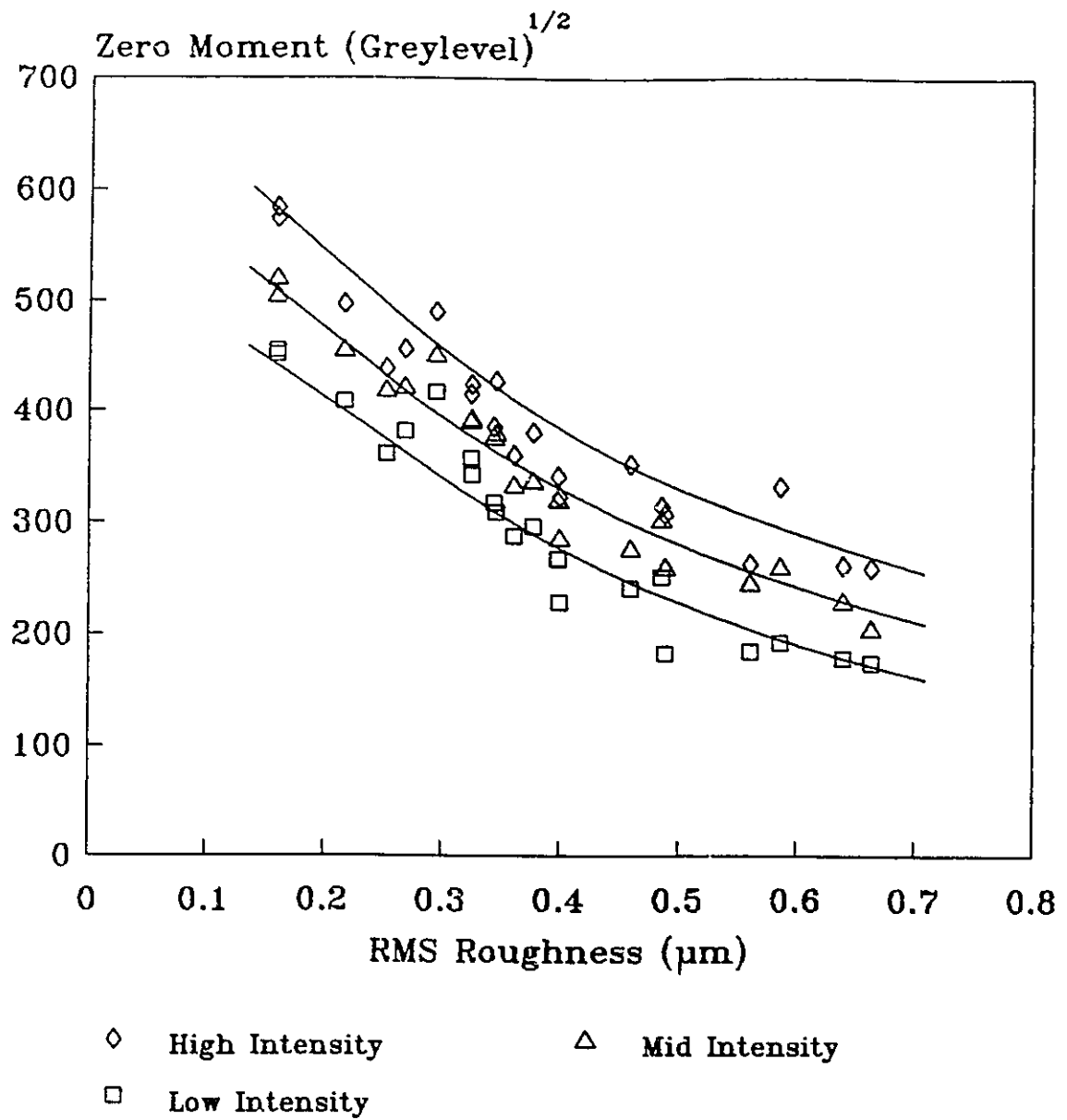
**Figure 5.8 Correlation curves of
RMS roughness for 2-D texture
surfaces on roller bearings**

Normalized Zero Moment vs RMS Roughness
2-D Texture Surfaces on Roller Bearings
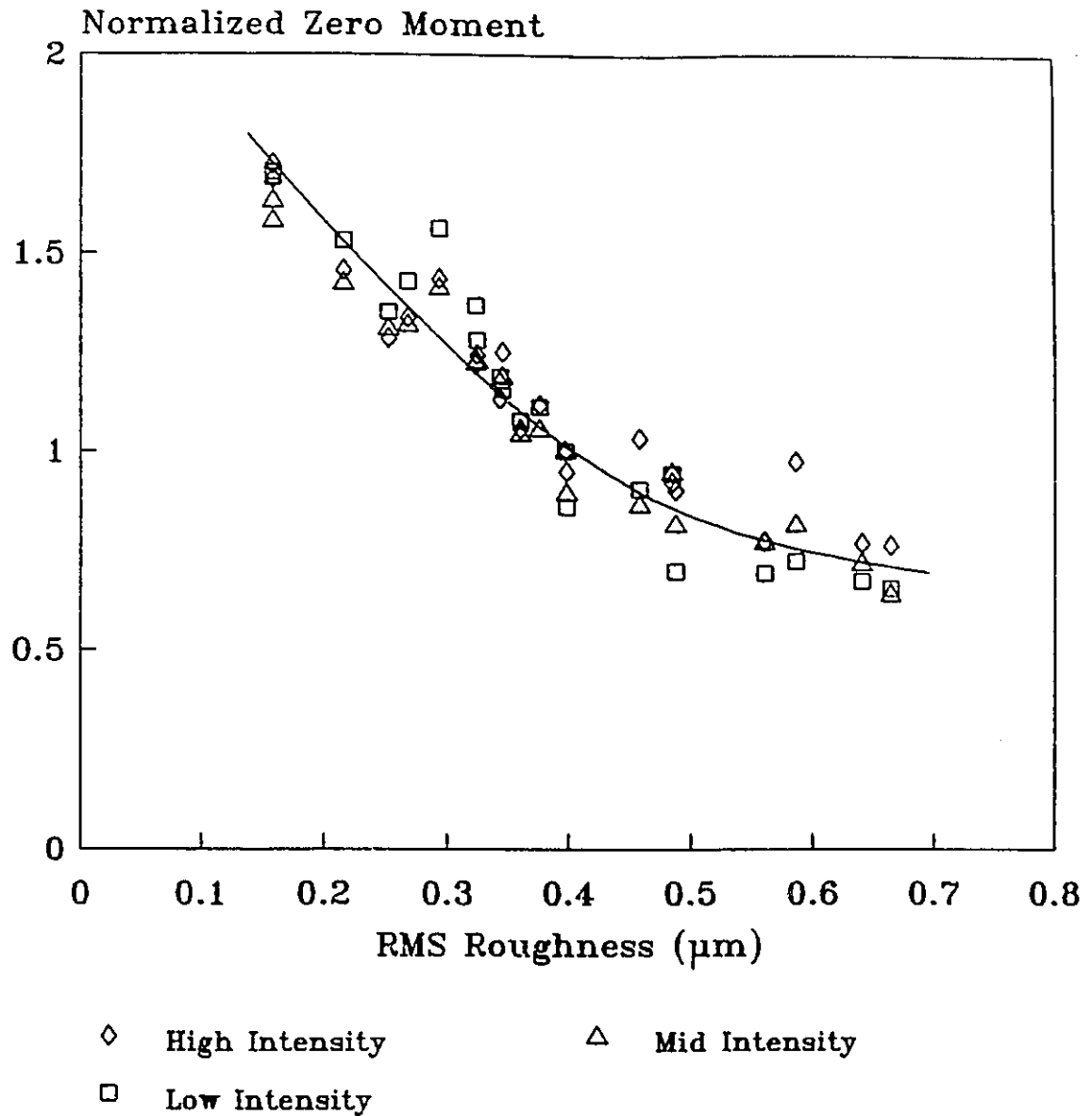
Figure 5.9 Normalized correlation curve
of RMS roughness for 2-D texture
surfaces on roller bearings

Normalized Zero Moment vs RMS Roughness 1&2D Texture Surfaces on Roller Bearings

Normalized Zero Moment

$$y = 1.79\ e^{-1.37x}$$
$$(r = -0.917)$$

RMS Roughness (μm)

1-D texture surfaces

2-D texture surfaces
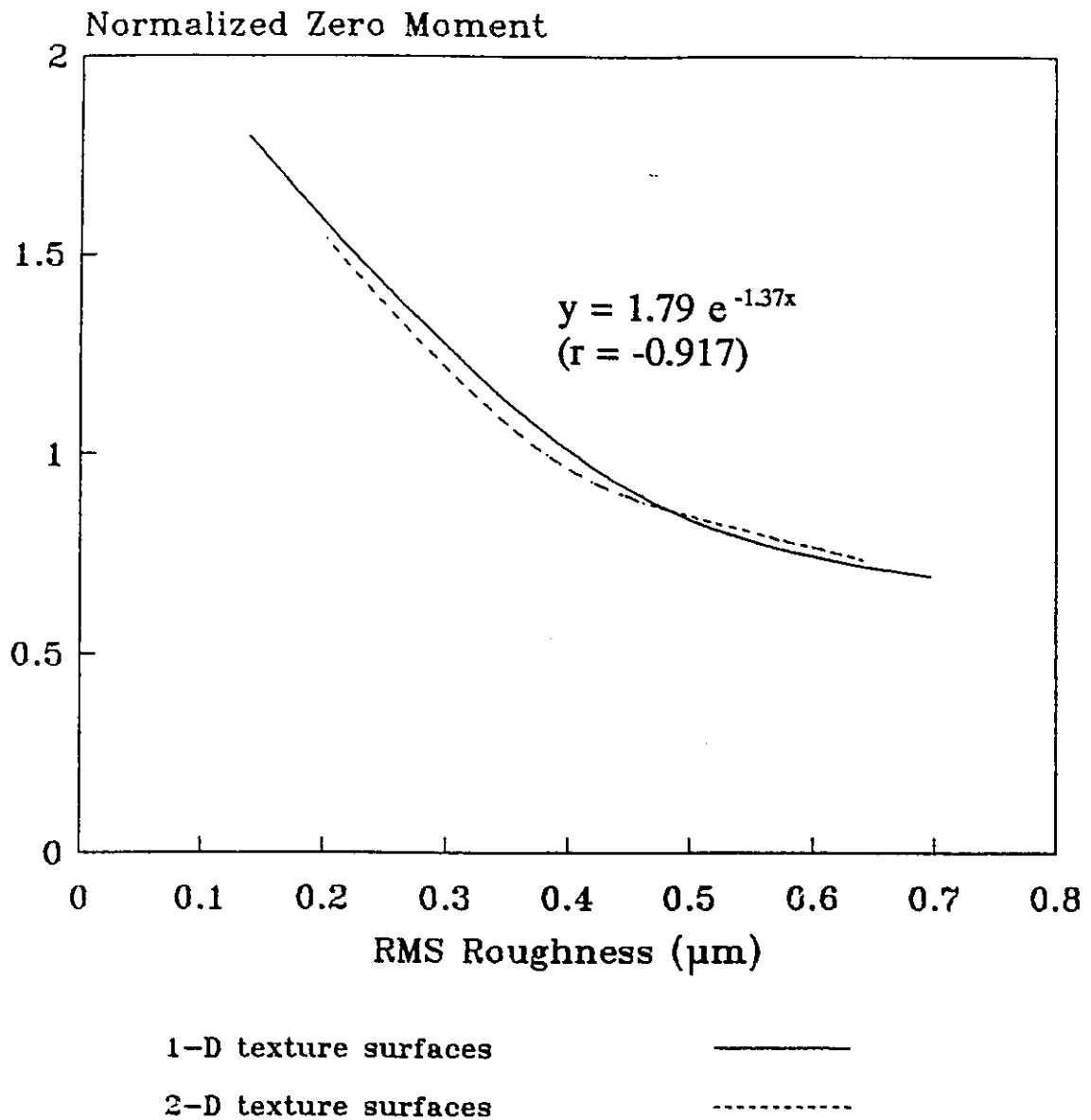
Figure 5.10 Normalized correlation curves of RMS roughness for 1-D & 2-D texture surfaces on roller bearings

. Second Moment vs RMS Slope
2-D Texture Surfaces on Roller Bearings
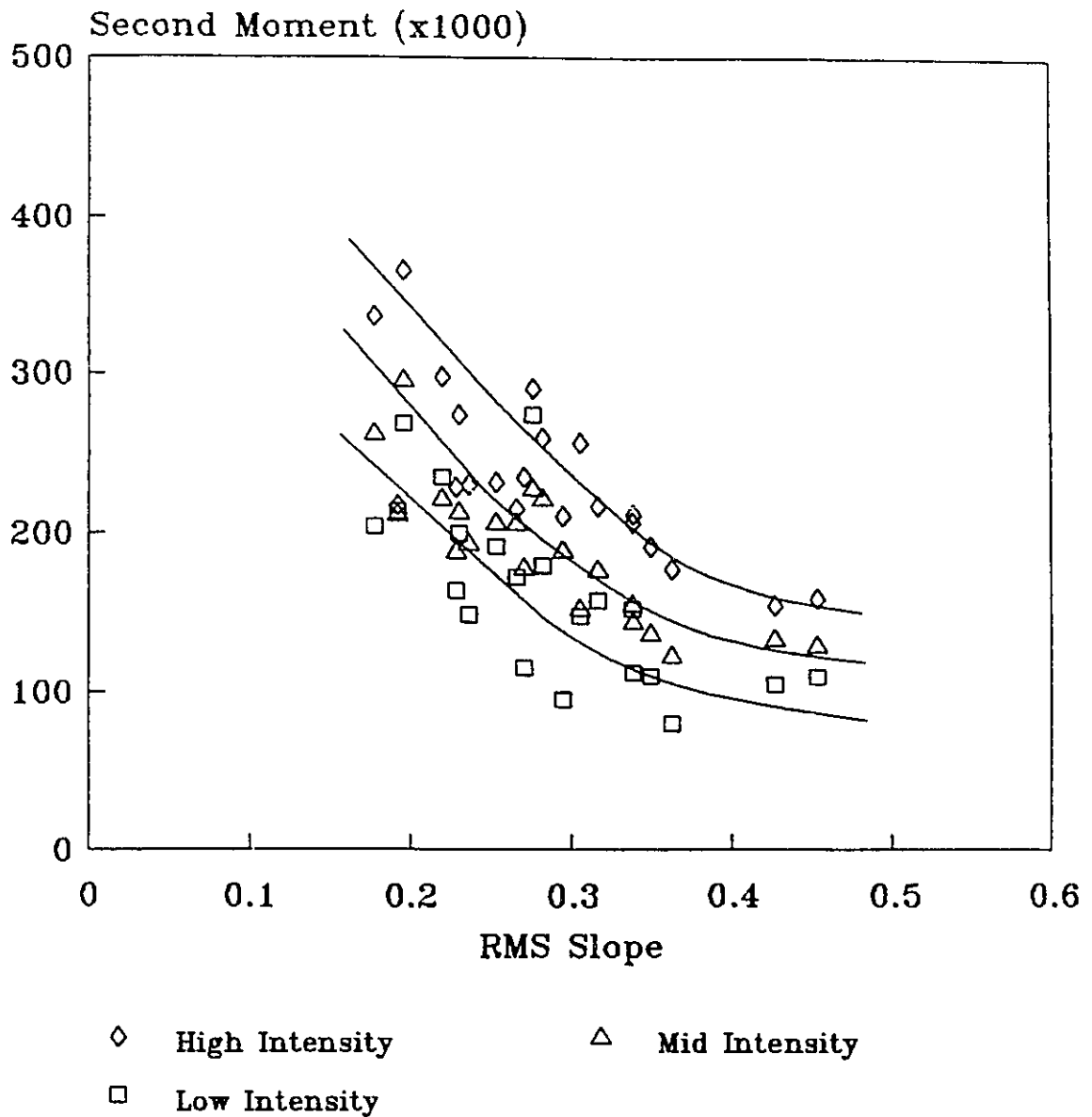
Figure 5.11 Correlation curves of
RMS slope for 2-D texture
surfaces on roller bearings

Normalized Second Moment vs RMS Slope
2-D Texture Surfaces on Roller Bearings
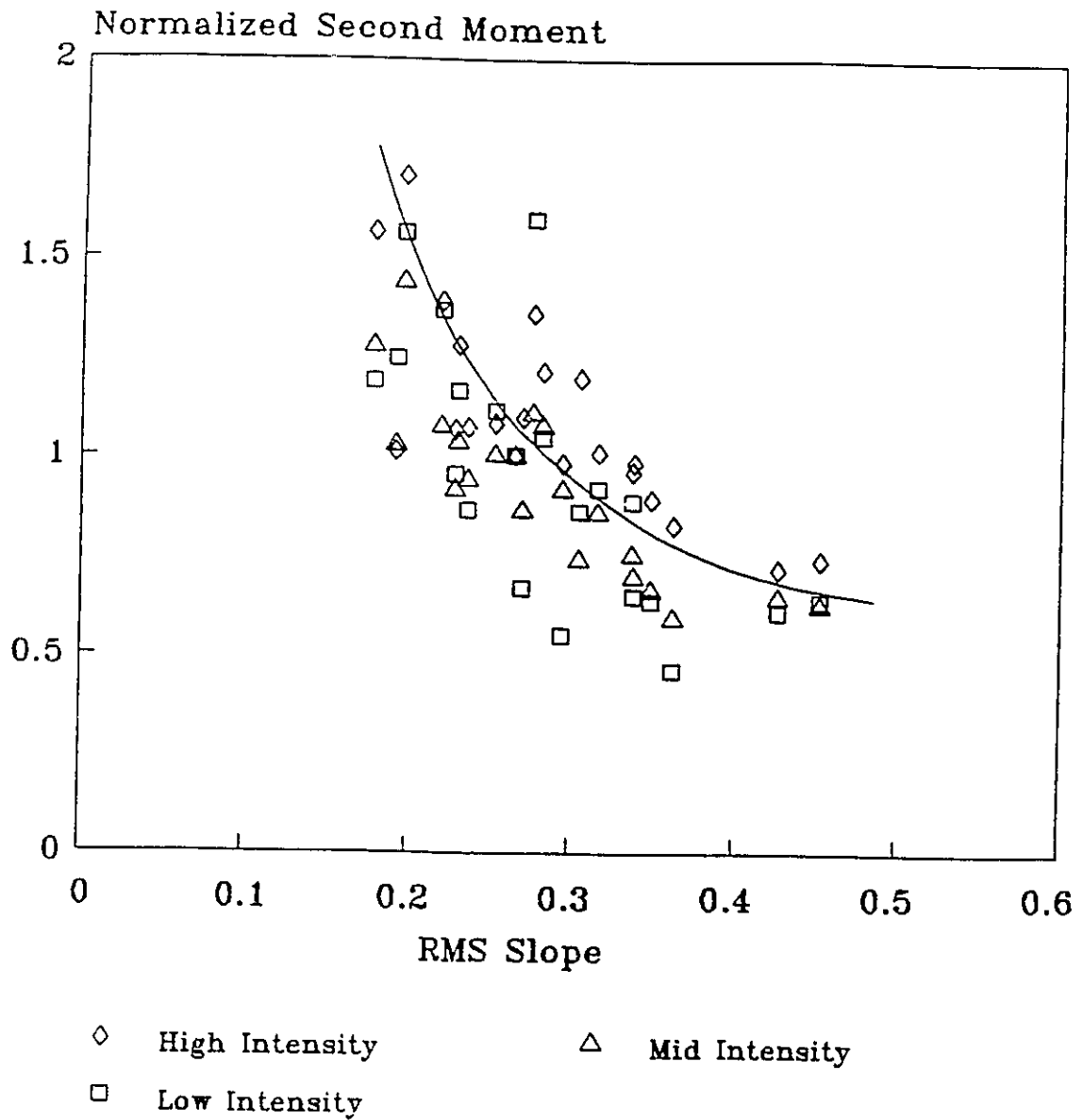
Figure 5.12 Normalized correlation
curve of RMS slope for 2-D texture
surfaces on roller bearings

81

Normalized Second Moment vs RMS Slope
2-D Texture Surfaces on Roller Bearings

Normalized Second Moment

$$y = 3.81 \, e^{-3.92x}$$
$$(r = -0.703)$$

$$y = 2.24 \, e^{-2.5x}$$
$$(r = -0.838)$$

RMS Slope

1-D texture surfaces ————

2-D texture surfaces ----------
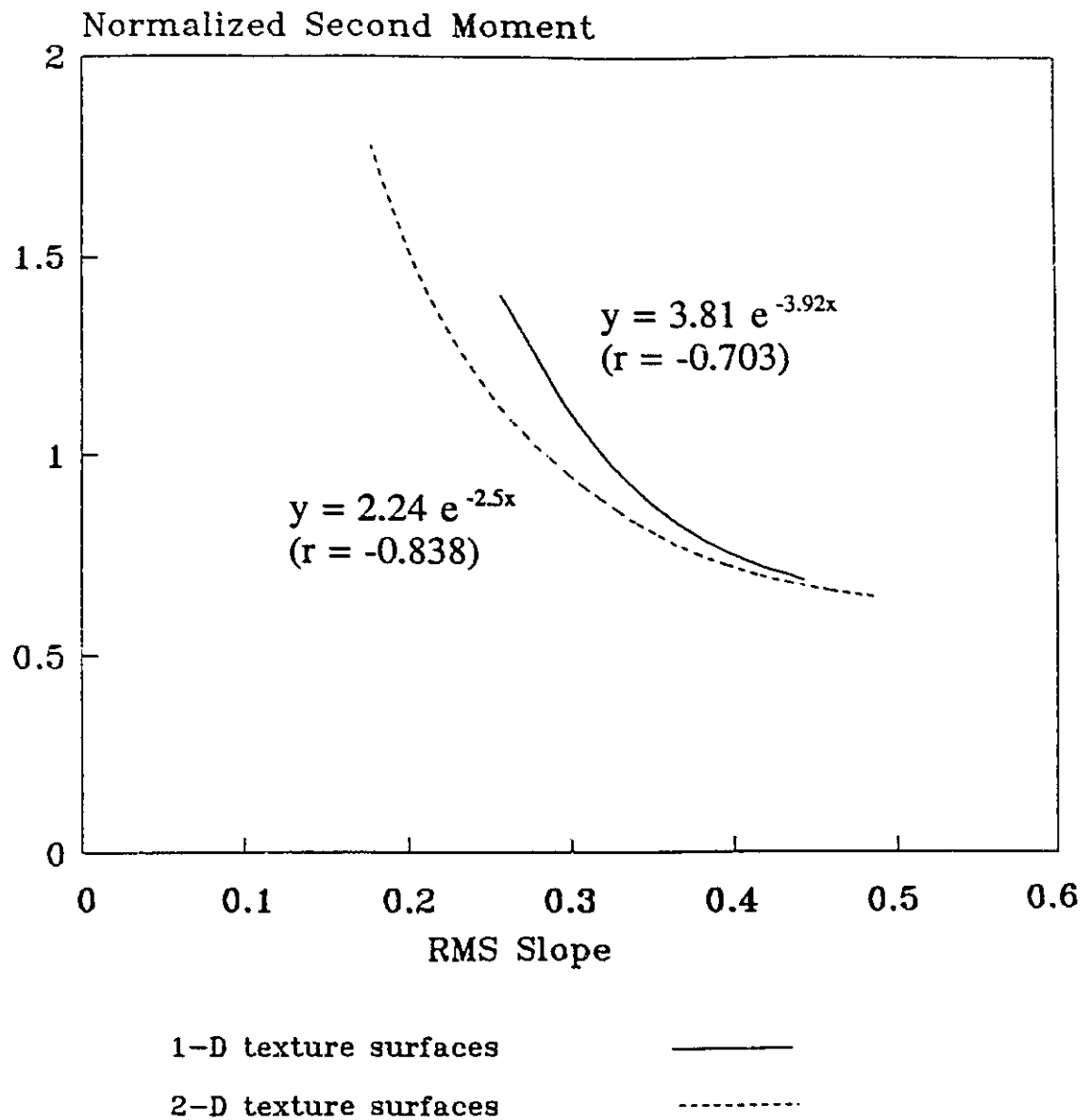
Figure 5.13 Normalized correlation
curves of RMS slope for 1-D & 2-D
texture surfaces on roller bearings

CHAPTER VI

CONCLUSIONS AND RECOMMENDATIONS

6.1 Conclusions

An optical measurement technique for the 2-D surface texture of roller bearings was developed. This technique is based on light (laser light) scattering from the surface. The bi-directional reflective distribution function (BRDF) of the scattering pattern of the surface was applied to derive the zero and second moments of the scattering pattern greylevel intensity as optical surface roughness parameters. The correlation of optical and mechanical roughness parameters was carried out for 1-D and 2-D texture surfaces of the bearings. From the results of the experiment, the following conclusions can be stated:

1) The optical measurement technique by light scattering for 1-D and 2-D surface texture roller bearings between 0.1 and 0.8 µm of mechanical RMS roughness was successfully developed.

2) Two optical roughness parameters, zero and second moments of the scattering pattern greylevel intensity, derived from the bi-directional reflective distribution function (BRDF), can be used to correlate to the mechanical RMS roughness and RMS slope, respectively.

3) Correlation curves were obtained to show the relationship between the optical parameters and the mechanical roughness parameters.

4) A common normalized correlation curve was established for 1-D and 2-D texture surfaces. Thus it is possible to establish one calibration curve for the evaluation

of either 1-D or 2-D texture surfaces. However, the type of texture must be known *apriori*. _

5) The possible relative error of the optical measurement is less than 10% on the average. This error may increase for rougher surfaces.

6) The orientation of the lay is not important in this measurement process for the range investigated.

6.2 Recommendations

Some factors should be considered to improve this measurement technique:

1) The range of mechanical RMS roughness of the sample surfaces can be extended (e.g. from 0.05µm to more than 1µm) in order to obtain the correlation curve(s) in the useful wider range.

2) The roller bearings used for this experiment were made of the same material. The effect of different material properties is not known. It would be of interest to take material property into account in this process.

3) A variety of 2-D texture surfaces (e.g. different angles between the two lay directions) can be used in the test to investigate the effect of lay angles.

4) Other roughness parameters such as skew or kurtosis for mechanical roughness parameters and third or higher order moments of the scattering patterns can be used as optical parameters for correlating with mechanical roughness parameters.

5) A specific optical surface can be selected as the standard surface for the normalization process instead of using a sample surface in order to standardize the normalization process for all types of surfaces.

6) Other factors affecting the measurement error, such as oxidized specimen surfaces or vibrations during measurements, should be considered. A more vigorous method of calculating the measurement uncertainty can also be established to determine the error in a more precise way.

7) Calibration of the camera can be carried out to ensure that it is linear and free of optical distortions.

REFERENCES

ANSI, 1978. "Surface Texture," American National Standards Institute, ANSI B46.1-1978, New York.

Asakura, T., 1978. "Surface Roughness Measurement" in Speckle Metrology: (R.K. Erf, editor), Academic Press, New York, Chapter 3, pp. 11 - 49.

Azzam, R.M.A. & Bashara, N.M., 1977. "Ellipsometry and Polarized Light," Amsterdam, Holland.

Beckmann, P. & Spizzichino, A., 1963. "The Scattering of Electromagnetic Waves from Rough Surfaces," Pergamon Press Ltd., New York.

Bendat, J.S. & Piersol, A.G., 1971. "Random Data: Analysis and Measurement Procedures," Wiely-Interscience, New York.

Bennett, J.M. & Mattsson, L., 1989. "Introduction to Surface Roughness and Scattering," Optical Society of America, Washington, D.C..

Blessing, G.V. & Eitzen, D.G., 1988. "Surface Roughness Sensed by Ultrasound," Surface Topography, pp. 143 - 158.

Brigham, E.O., 1974. "The Fast Fourier Transform," Prentice-Hall, Inc., New Jersey.

Brodmann, R. & Thurn, G., 1986. "Roughness Measurement of Ground, Turen and Shot-Peened Surfaces by the Light Scattering Methods," Wear, Vol. 109, pp. 1 - 13.

Brodmann, R. & Allgauer, M., 1988. "Comparison of Light Scattering from Rough Surfaces with Optical and Mechanical Profilometry," Proceedings of the SPIE. Vol. 1009, pp. 111 - 118.

Chandley, P.J., 1976. "Determination of the Autocorrelation Function of Height on a Rough Surface from Coherent Light Scattering," Optical and Quantum Electronics, Vol. 8, pp. 329 - 333.

Chu, B., 1991. "Laser Light Scattering - Basic Principles and Practice," 2nd Ed., Academic Press, Inc., New York.

Cogdell, J.D., 1987. "PhD Thesis: Theoretical and Experimental Correlations Between Surface Topography and Tribological Functionality," Rensselaser Polytechnic Insutute, Troy, New York.

Cuthbert, L., 1991. "Master's Thesis: Surface Texture Assessment by Statistical Analysis of Optical Fourier Transform Patterns," University of Windsor, Windsor, Canada.

Dai, Y.Z. & Chiang, F.P., 1991. "Scattering from Plastically Roughened Surfaces and Its Applications to Strain Assessment," Optical Engineering, pp. 1269 - 1276, September.

Duffieux, P.M., 1983. "The Fourier Transform and Its Applications to Optics," 2nd Ed., John Wiley & Sons, New York.

Fujii, H. & Asakura, T., 1977. "Roughness Measurement of Metal Surfaces Using Laser Speckle," Journal of the Optical Society of America, Vol. 67, No. 9, pp. 1171 - 1176.

Garbini, L.J., Albrecht, L.J., Jorgensen, J.E. & Mauer, G.F., 1985. "Surface Profilometry Based on Fringing Capacitance Measurement," ASME Journal of Dynamic System, Measurement, and Control, Vol. 107, pp. 192 - 199.

Halliday, D. & Resnick, R., 1978. "Physics," 3rd Edition, John Wiley & Sons, New York.

Hariharan, P., 1985. "Optical Interferometry," Academic Press, North Ryde, Australia, 1985.

Huynh, V., Cuthbert, L. & Kurada, S., "Application of Machine Vision to Surface Texture Measurement," Vision 90 Conference Proceedings, Machine Vision Association of the Society of Manufacturing Engineers. pp. 8-17 - 8-30.

Huynh, V. & Fan, Y., 1991. "Surface Texture Measurement and Characterization with Applications to Machine Tool Monitoring," University of Windsor, Windsor, Canada, 1991.

Huynh, V., North, W. & Luk, F., 1989. "Contributed Papers: Measurement of Surface Roughness by a Machine Vision System," J. Phys. E.: Science Instrument, IOP Publishing Ltd., U.K., pp. 977 - 980.

Kruger, J. & Hayfield, P.C.S., 1971. "Ellipsometry in Corrosion Testing," in Handbook of Corrosion Testing and Evaluation (W.H. Ailor, ed.), John Wiley and Sons, New York.

Kurada, S., 1988. "Master's Thesis: Study of Surface Texture Using Fourier Transform Methods," University of Windsor, Windsor, Canada.

Lonardo, P.M., 1974. "Measurement of Smooth Surface Roughness by Means of a Photometric Method," CIRP Annals, Vol. 23, p. 189.

Lonardo, P.M., 1978. "Testing a New Optical Sensor for In-Process Detection of Surface Roughness," CIRP Annals, Vol. 27, p. 531.

Luk, F., 1987. "Master's Thesis: A Vision System for Surface Roughness Measurement," University of Windsor, Windsor, Canada.

Morgan, J., 1953. "Introduction to Geometrical and Physical Optics," McGraw-Hill Book Co., Inc., New York.

Nicodem, F.E., Richmond, J.C., Hsia, J.J., Ginsberg, I.W. & Limperis, T., 1977. "Geometric Considerations and Nomenclature for Reflectance," U.S. Department of Commerce, Washington, D.C., NBS Monograph.

Rakels, J.H., 1988. "Recognized Surface Finish Parameters Obtained from Diffraction Patterns of Rough Surfaces," Proceedings of the SPIE. Vol. 1009 , pp. 119 - 125.

Rice, S.O., 1951. "Communication Pure Applied Math.," Vol. 4, p. 351.

Sasaki, O. & Fukuhara, Y., 1985. "Surface Profile Measurement from Intensity of Diffracted Light Using the Phase Retrieval Method," Applied Optics, Vol. 26, No. 12, 15 June.

Sommargren, G.E., 1981. "Optical Heterodyne Profilometry," Applied Optical, Vol.20, No. 4, February 15, pp. 610-618.

Stover, J.C., 1990. "Optical Scattering: Measurement and Analysis," McGraw-Hill, Inc., U.S.A..

Tenoudji F.C. & Quentin, G., 1982. "Characterization of Surfaces by Deconvolution of Ultrasonic Echoes Using Extended Bandwidth," Journal of Applied Physics, Vol. 53, pp. 4057 - 4063.

Thomas, T.R., 1982. "Rough Surfaces," Longman Inc., U.S.A..

Vorburger, T.V. & Ludema, K.C., 1980. "Ellipsometry of Rough Surfaces," Applied Optics, Vol. 19, p. 561.

88

APPENDIX A

EQUIPMENT SPECIFICATIONS

Stylus Instrument

Manufacturer : Mitutoyo Manufacturing Co., Ltd., Japan

Model : Surfest III

Tip radius : 10 μm $\pm$ 2.5 μm

Tip angle : 90° $\pm$ 10°

Skid radius : 15 mm

Traverse speed : 2 mm/s or 6mm/s

He-Ne Laser

Manufacturer : Opticon

Model : LM2P, Class IIIb Laser product

Wavelength : 632.8 nm

Beam diameter : 0.75mm at $1/e^2$

Maximum output power : 5 mW

Operating Temperature : -20°C to +50°C

High resolution monitor

Manufacturer : Panasonic, Matsushita Co., Ltd.

Model : WV-5410

CCD Camera .

Manufacturer : NEC Co., Japan.

Model : TI-23A

Image cell size : 16 μm × 20 μm

Image size : 4.84 mm × 6.45mm

Signal system : EIA standards Rs-170

Signal to noise ratio : 60 dB

Size (H × W × L) : 75 mm × 114 mm × 235 mm

Digitizing Board

Manufacturer : MATROX Electronic System Ltd., Canada.

Model : PIP-1024

Resolution 512 × 512 pixels

Grey level : 256 (8 bits)

Image Store : One 1024 × 1024 buffer or
              four 512 × 512 buffers

D/A Converters : Three 8 bit D/A converters for RGB input

Output : 8 bits in / 24 bits out

Size (H × W × L) : 335.3 mm × 106.8 mm × 32.7 mm

APPENDIX B

DATA FOR CORRELATION CURVES

Table B.1   Data for the zero moment vs RMS roughness of 1-D
            texture sample surfaces

Sample Surface	Mechanical RMS Roughness (μm)	Optical Zero Moment (Greylevel)$^{1/2}$		
		Laser Intensity:		
		High	Mid	Low
A5	0.258	606	470	323
B5	0.265	601	457	325
B1	0.370	530	405	249
A1	0.382	474	352	222
B6	0.390	494	384	232
A6	0.400	488	359	214
B3	0.417	479	347	243
A3	0.434	483	311	206
B2	0.447	445	324	186
A2	0.491	425	319	155
B4	0.510	431	308	158
A4	0.584	417	308	158

Table B.2   Data for the normalized zero moment vs RMS roughness of
            1-D texture sample surfaces

Sample Surface	Mechanical RMS Roughness (µm)	Normalized Optical Zero Moment		
		Laser Intensity:		
		High	Mid	Low
A5	0.258	1.28	1.33	1.45
B5	0.265	1.27	1.30	1.46
B1	0.370	1.12	1.16	1.12
A1	0.382	1.00	1.00	1.00
B6	0.390	1.04	1.09	1.04
A6	0.400	1.03	1.02	0.96
B3	0.417	1.01	0.99	1.10
A3	0.434	1.02	0.92	0.93
B2	0.447	0.94	0.88	0.84
A2	0.491	0.90	0.91	0.70
B4	0.510	0.91	0.88	0.71
A4	0.584	0.88	0.88	0.55

Table B.3   Data for the second moment vs RMS slope of 1-D texture
            sample surfaces

Sample Surface	Mechanical RMS Slope	Optical Second Moment ($\times 1000$)		
		Laser Intensity:		
		High	Mid	Low
B5	0.268	431	314	222
A5	0.272	452	337	215
B1	0.300	336	264	140
A1	0.306	341	248	174
A3	0.306	386	222	113
B3	0.316	332	242	179
B2	0.321	331	198	122
A6	0.331	322	230	119
B6	0.341	326	221	141
A2	0.385	308	210	91
A4	0.395	308	202	74
B4	0.410	305	228	96

Table B.4   Data for the normalized second moment vs RMS slope of
            1-D texture sample surfaces

Sample Surface	Mechanical RMS Slope	Normalized Optical Second Moment		
		Laser Intensity:		
		High	Mid	Low
B5	0.268	1.26	1.26	1.28
A5	0.272	1.33	1.36	1.24
B1	0.300	0.99	1.06	0.88
A1	0.306	1.00	1.00	1.00
A3	0.306	1.14	0.89	0.65
B3	0.316	0.97	0.93	1.03
B2	0.321	0.97	0.80	0.70
A6	0.331	0.95	0.93	0.69
B6	0.341	0.96	0.89	0.82
A2	0.385	0.92	0.85	0.52
A4	0.395	0.90	0.82	0.43
B4	0.410	0.90	0.92	0.55

Table B.5   Data for the zero moment vs RMS roughness of 2-D
texture sample surfaces

Sample Surface	Mechanical RMS Roughness (μm)	Optical Zero Moment (Greylevel)$^{1/2}$		
		Laser Intensity:		
		High	Mid	Low
E5	0.159	584	526	450
F5	0.159	574	503	453
D5	0.216	497	454	408
E1	0.252	438	417	360
D1	0.268	456	421	381
D3	0.294	489	450	417
F1	0.324	415	389	356
C5	0.325	423	392	341
F3	0.344	385	375	317
E3	0.346	427	379	309
E2	0.361	360	332	287
D2	0.377	380	336	296
C1	0.398	341	301	251
F2	0.399	323	285	229
E4	0.459	352	275	241
C3	0.485	314	301	251
C6	0.488	307	259	183
C2	0.560	263	245	185
F4	0.586	332	260	192
D4	0.640	261	229	179
C4	0.664	259	204	174

Table B.6   Data for the normalized zero moment vs RMS roughness of
            2-D texture sample surfaces

Sample Surface	Mechanical RMS Roughness (μm)	Normalized Optical Zero Moment		
		Laser Intensity:		
		High	Mid	Low
E5	0.159	1.72	1.63	1.69
F5	0.159	1.68	1.58	1.70
D5	0.216	1.46	1.42	1.53
E1	0.252	1.28	1.31	1.35
D1	0.268	1.34	1.32	1.43
D3	0.294	1.44	1.41	1.56
F1	0.324	1.22	1.22	1.37
C5	0.325	1.24	1.23	1.28
F3	0.344	1.13	1.18	1.19
E3	0.346	1.25	1.19	1.16
E2	0.361	1.06	1.04	1.08
D2	0.377	1.12	1.05	1.11
C1	0.398	1.00	1.00	1.00
F2	0.399	0.95	0.89	0.86
E4	0.459	1.03	0.86	0.90
C3	0.485	0.92	0.95	0.94
C6	0.488	0.90	0.91	0.70
C2	0.560	0.77	0.77	0.69
F4	0.586	0.97	0.81	0.70
D4	0.640	0.77	0.71	0.67
C4	0.664	0.76	0.64	0.65

Table B.7   Data for the second moment vs RMS slope of 2-D texture
            sample surfaces

Sample Surface	Mechanical RMS Slope	Optical Second Moment ($\times 1000$)		
		Laser Intensity:		
		High	Mid	Low
F5	0.118	335	262	203
E1	0.192	217	211	213
E5	0.196	365	295	268
D5	0.220	297	221	234
F1	0.229	228	188	163
D1	0.230	273	212	199
E3	0.236	229	193	148
F3	0.253	231	206	190
C1	0.266	214	205	171
D2	0.270	234	177	115
D3	0.276	290	227	274
C5	0.282	259	220	179
F2	0.294	210	188	94
E4	0.305	256	152	147
E2	0.316	216	176	157
C3	0.337	205	154	152
C6	0.338	211	143	111
F4	0.349	191	136	109
C4	0.362	177	122	80
C2	0.427	154	133	104
D4	0.453	158	129	109

Table B.8   Data for the normalized second moment vs RMS slope of
            2-D texture sample surfaces

Sample Surface	Mechanical RMS Slope	Optical Second Moment (×1000)		
		Laser Intensity:		
		High	Mid	Low
F5	0.118	1.56	1.27	1.18
E1	0.192	1.01	1.03	1.24
E5	0.196	1.70	1.44	1.56
D5	0.220	1.39	1.07	1.37
F1	0.229	1.06	0.91	0.95
D1	0.230	1.28	1.04	1.16
E3	0.236	1.35	1.10	1.60
F3	0.253	1.08	1.00	1.11
C1	0.266	1.00	1.00	1.00
D2	0.270	1.09	0.86	0.67
D3	0.276	1.35	1.11	1.60
C5	0.282	1.21	1.08	1.04
F2	0.294	0.98	0.92	0.55
E4	0.305	1.19	0.74	0.86
E2	0.316	1.01	0.86	0.92
C3	0.337	0.96	0.75	0.88
C6	0.338	0.98	0.70	0.65
F4	0.349	0.89	0.66	0.63
C4	0.362	0.83	0.60	0.46
C2	0.427	0.72	0.65	0.61
D4	0.453	0.74	0.63	0.64

Table B.9   Data for the measurement precision of the optical technique
by using C1 sample surfaces

(a) Error due to focusing

Number of Measurement	Zero Moment (Greylevel)$^{1/2}$	Second Moment ($\times 1000$)
1	345	179
2	334	180
3	348	180
4	358	186
5	341	186

(b) Error due to centering

Number of Measurement	Zero Moment (Greylevel)$^{1/2}$	Second Moment ($\times 1000$)
1	371	187
2	356	164
3	326	159
4	335	156
5	345	162

(c) Error due to Surface Non-uniformity

Number of Measurement	Zero Moment (Greylevel)$^{1/2}$	Second Moment ($\times 1000$)
1	343	192
2	371	193
3	376	186
4	390	174
5	383	194

APPENDIX C

COMPUTER PROGRAM LIST

```
$include:'forintf.h'

c       mainline program

c       ******************************************
c       *          Declaration Statements        *
c       ******************************************
        implicit integer (a-e)
        implicit real*4 (f)
        implicit integer*2 (g-z)
        real*4 cv,s2,mean,data1(250),data2(250),data3(250),freq(250)
        real*4 slope,sum1,sum2,sum3,rms,fdata,xdata,rmss,xa,ya
        real*8 sx,sy,fpr,fi,fj,fir,sec,s
        integer*2 x(20),y(20),prof(1024),prof1(1024),x1,y1,quad
        integer*2 ifirst,iave,i1,i2,left,right,pr
        integer*2 wx1,wx2,wx3,wx4,wy1,wy2,wy3,wy4,wd,ww,m1,n1
                integer*4 vol
c       ***** offset and gain *****
        integer*4 off,gn
        character*20 tx1,tx2
        character*10 cmx
        character*3 cmax,res
        character*2 ca
        character*13 fname
        character*20 fname1,fname2,fname3
        character  dum,buf1(512),buf2(512),buf(512),buffer(4096),
        workbuffer(512),dumy,ask

c       ******************************************
c       *          initialization of the board   *
c       ******************************************
        ir=init(620)
        if (ir.ne.1) write (*,*)ir
        call chan(2)
        call video (0)
        call sync(0)
c       ***** setting offset and gain *****
        off=70
        gn=120
        call offset(off)
        call gain(gn)
c       PIP-1024 mode
        call quadm(1)
c       display quadrant 0
        call dquad(0)
```

```
        write(*,997)
997     format(////,t6,'NOTE:THE DISPLAYED QUADRANT IS 0'./,
    *                        t6,'    CAMERA IS OFF'.//,
    *                   t6,'HIT <ENTER> FOR MAIN MENU'./)
        read(*,'(a1)') dumy
           bsize=4096


4       write(*,5)
5       format('1'./,t6,'IMAGE PROCESSING ROUTINES './,
    *          t6,'------------------------'./)
        write(*,10)
10      format(//,  t6,' 0. CAMERA ON/OFF'./,
    *              t6,' 1. CONTINUOUSGRAB/SNAPSHOT'./,
    *          t6,' 2. SAVE/LOAD A PICTURE './,
    *          t6,' 3. SELECT THE QUADRANT TO BE DISPLAYED/CLEARED'./,
    *          t6,' 4. POINT PIXEL READ'./,
    *          t6,' 5. GREYLEVEL PROFILE './,
    *          t6,' 6. HISTOGRAM ANALYSIS'./,
    *              t6,' 7. FAST FOURIER TRANSFORM ANALYSIS'./,
    *          t6,' 8. SET OFFSET AND GAIN'./,
    *          t6,' 9. ADDING TWO IMAGES (QUAD 1 + QUAD 2 --> QUAD 3)'./,
    *          t6,' './,
    *          t6,'10. COPY IMAGE (FROM QUAD X TO QUAD Y)'./,
    *              t6,'11. *****                './,
    *              t6,'12. CALCULATE RMS & SLOPE OF PATTEN'./,
    *              t6,'13. MATCH QUAD 1 & 2 TO QUAD 0'./,
    *              t6,'14. EXIT PROGRAM'./)

        read(*,'(i2)')num


c       *******************
c       *    camera on/off      *
c       *******************
        if(num.ne.0) go to 662
        cam=0
        write(*,1)
1       format(/,T6,'CAMERA ON/OFF ? (ON/OFF) './)
        read(*,'(a2)')ca
        if(ca.eq.'ON'.or.ca.eq.'on')cam=1
        call sync (cam)

662     if(num.ne.6) go to 117
c       *****************************
c       *           histogram analysis          *
c       *****************************
```

104

```fortran
      write(*,200)
200   format('1',/,t6,'HISTOGRAM ANALYSIS',/,
     *          . t6,'-------------------',/)
      write(*,911)
911   format(/,t6,'QUADRANT ? (0-3)',/)
      read(*,'(i2)')iquad
      call ghist(iquad)
      go to 4


117   if(num.ne.7) goto 15
c     ****************************
c     *            f.f.t analysis            *
c     ****************************
      write(*,777)
777   format('1',/,t6,'F.F.T ANALYSIS',/,
     *                  t6,'--------------',/)
      write(*,911)
      read(*,'(i2)')iquad
      call dquad(iquad)
      call crsr(x1,y1,x2,y2,quad)
      call setwin(x1,y1,x2,y2)
      call fftanaly(x1,y1,x2,y2,iquad)
      go to 4


15    if(num.ne.1) go to 20
c     ******************************
c     *       continuous grab/snapshot       *
c     ******************************
c     checking for camera on off state
      if (cam.eq.0) goto 4
      write(*,666)
666   format('1',t6,'CONTINUOUS GRAB/SNAPSHOT',/,
     *          t6,'--------------------------',/)
      call cgrab(1)
      write(*,*)'   HIT <ENTER> TO GRAB PICTURE'
      read(*,'(a1)')ask
      call cgrab(0)


20    if(num.ne.2) go to 30
c     *************************
c     *      save or load picture    *
c     *************************
      write(*,210)
210   format('1',T6,'SAVE/LOAD ? (S/L) ; QUADRANT ? (0-3)',/)
      read(*,771)ask,iquad
```

```
771      format(a1,i2)
         write(*,215)
215      format(/,t6,'FILENAME ? (DRIVER:\PATH\FILENAME)',/)
         read(*,'(a13)')fname
         call dquad(iquad)


c        ****** loading picture ******
         if(ask.eq.'L'.or.ask.eq.'l') then
         iret=ifrdsk(bsize,iquad,fname,workbuffer)


c        ****** saving picture *******
         else if(ask.eq.'S'.or.ask.eq.'s') then
         iret=itodsk(bsize,iquad,fname,buffer)


c        ****** in case of typing error *******
         else
         go to 4
         end if


         if(iret.eq.1)then
         write(*,216)
216      format(/,T6,'TRANSFER COMPLETED',/)
         else if(iret.eq.0) then
         write(*,217)
217      format(/,t6,'COULD NOT OPEN FILE',/)
         else if(iret.eq.-1) then
         write(*,218)
218      format(/,t6,'DISK ERROR',/)
         end if
         go to 4


30       if (num.ne.5) goto 40
c        ***********************
c        *     greylevel profile      *
c        ***********************
         write(*,444)
444      format('1',/,t6,'GREYLEVEL PROFILE',/,
     *          t6,'----------------',/)
         cmx='max value='
         write(*,911)
         read(*,'(i2)')iquad
         call dquad(iquad)
         write(*,351)
351      format(/,t6,'1. HORIZONTAL PROFILE',/,
     *          t6,'2. VERTICAL PROFILE ',/,
```

106

```
    *        t6,'3. TWO POINTS FORM  X-DIR  (QUAD 0 ONLY)'./,
    *        t6,'4. TWO POINTS FORM  Y-DIR  (QUAD 0 ONLY)'./)
             read(*,'(j2)')num1
             call profile(iquad,num1)

c        ***********************
c        *     point pixel read     *
c        ***********************
40       if (num.ne.4) go to 50
         write(*,888)
888      format('1'./,t6,'POINT PIXIL READ'./,
    *               t6,'----------------'./)
         write(*,911)
         read(*,'(i2)')iquad
         call dquad(iquad)
         dx=0
         dy=0
         if(iquad.eq.2.or.iquad.eq.3) dx=512
         if(iquad.eq.1.or.iquad.eq.3) dy=512

c        ***** drawing initial cursor *****

         xr=256+dx
         yr=240+dy
         j=0
         do 35 i=xr-8,xr+8
         j=j+1
         x(j)=ipixr(i,yr)
         call pixw(i,yr,255)
35       continue
         j=0
         do 36 i=yr-8,yr+8
         j=j+1
         if (j.eq.9) then
         y(j)=x(j)
         else
         y(j)=ipixr(xr,i)
         endif
         call pixw(xr,i,255)
36       continue

c        cursor displacement
         idl=3
         write(*,370)
370      format(/,t6,'MOVE CURSOR TO THE POINT OF INTEREST,',
```

```
*        /,t6,'HIT <RETURN> FOR MAIN MENU'/)
39       ipnt=x(9)
         write(*,372)ipnt
372      format('+',t5,i4)
         dir=getkey(ii)
         if (dir.eq.274.or.dir.eq.275.or.dir.eq.276.or.dir.eq.277) then
         yref=yr
         xref=xr
         if (dir.eq.274) yr=yr-idl
         if (dir.eq.275) yr=yr+idl
         if (dir.eq.276) xr=xr-idl
         if (dir.eq.277) xr=xr+idl
         do 37 i=1,17
         call pixw(xref-9+i,yref,x(i))
         call pixw(xref,yref-9+i,y(i))
37       continue
         do 61 i=1,17
         x(i)=ipixr(xr-9+i,yr)
         y(i)=ipixr(xr,yr-9+i)
         call pixw(xr-9+i,yr,255)
         call pixw(xr,yr-9+i,255)
61       continue
         elseif(dir.eq.13) then
         do 38 i=1,17
                 call pixw(xr-9+i,yr,x(i))
                 call pixw(xr,yr-9+i,y(i))
38       continue
         goto 50
         endif
         goto 39

50       if(num.ne.3) go to 510
c        ************************************************
c        *     select the quadrant to be displayed/cleared *
c        ************************************************
         write(*,222)
222      format('1'/,t6,'SELECT THE QUADRANT TO BE DISPLAYED/CLEARED',
*            /,t6,'----------------------------------------',/)
         write(*,556)
556      format(/,t6,'DISPLAY/CLEAR ? (D/C) ; QUADRANT ? (0-3)',/)
         read(*,772)ask,iquad
772      format(a1,i2)
         call dquad(iquad)
         if(ask.eq.'c'.or.ask.eq.'C')then
         call setind(255)
```

```
            call clear(0,7)
            end if

510     if(num.ne.8) goto 70
c       ***********************
c       *  set offset and gain  *
c       ***********************
            write(*,520)
520     format('1',/,t6,'SET OFFSET AND GAIN',/,
        *           t6,'-------------------',/)
c     ***** setting offset *****
            write(*,530)off
530     format(/,t6,'SET OFFSET (0 TO 255): ',i4)
            read(*,'(i4)')off
            call offset(off)
c***** setting gain
            write(*,540)gn
540     format(/,t6,'SET GAIN (0 TO 255): ',i4)
            read(*,'(i4)')gn
            call gain(gn)

70      if(num.ne.9) goto 80
c       ***********************
c       *   adding two images   *
c       ***********************
            call dquad(3)
            call setind(255)
            call clear(0,7)
            x1=0
            y1=0
            z1=0
            do 910 k=1,512
            call rowr(x1,1,buf1)
            call rowr(x1,2,buf2)
            do 900 i=1,512
            i1=ichar(buf1(i))
            i2=ichar(buf2(i))
            if (i1.ge.i2) i3=i1
            if (i2.ge.i1) i3=i2
            buf(i)=char(i3)
900     continue
            call roww(z1,3,buf)
            x1=x1+1
            y1=y1+1
            z1=z1+1
```

```
910     continue


80      if (num.ne.10) goto 60
c       ******************
c       *   copy image   *
c       ******************
        print*,' '
        print*,' '
        print*,'   COPY FROM QUAD ?  (0-3)'
        read(*,'(i1)')cf
        print*,' '
        print*,'   COPY TO QUAD ?  (0-3)'
        read(*,'(i1)')ct
        print*,' '
        do 85 i=1,512
        call rowr(i,cf,buf)
        call roww(i,ct,buf)
85      continue
        call dquad(ct)
        print*,' '
        print*,' '
        print*,' '
        write(*,86) ct
86      format(' DONE !  QUADRANT ',i1,' IS NOW ON THE SCREEN')


60      if (num.ne.11) goto90
c       *************************************
c       *     calculate rms & m of profile     *
c       *************************************

c       ***** initialization of the paramaters *****
        DO 140 i=1,250
        data1(i)=0.0
        data2(i)=0.0
        freq(i)=0.0
140     continue

c   ***** read data file *****
        write (*,150)
150     format(/,t6,'FILENAME ?  (DRIVER:\PATH\FILENAME)')
        read(*,'(a20)')fname1
        write (*,155)
155     format(/,t6,'NO. OF DATA IN THE FILE  (MAX. 230) ?')
```

```
        read(*,'(i4)')idata
        open(unit=10,file=fname1,status='old')
        do 160 i=1,idata
                read(10,165)data1(i),data2(i)
165             format(f10.4,f10.0)
160     continue
        close(unit=10,status='keep')


c       ***** calculate mean *****
        do 170 i=1,idata
                fdata=data2(i)
                sum1=data1(i)*data2(i)
                sum2=sum2+data2(i)
                sum3=sum3+sum1
170     continue
        mean=sum3/sum2


c       ***** reform data *****
c       (into spatial freq. in c/mm vs. spectrum intensity)
        write(*,180)
180     format(/,t6,'FACTOR = ?',/)
        read(*,'(f12.9)')factor
        do 185 i=1,idata
        freq(i)=(data1(i)-mean)*1.70333333*factor
185     continue


c       ***** write reformed data to new file ****
        write(*,187)
187     format(/,t6,'NEW FILENAME ?')
        read (*,'(a20)')fname2
        open(unit=10,file=fname2,status='new')
        do 190 i=1,idata
                write(10,195)freq(i),data2(i)
195             format(f10.4,f10.0)
190     continue
        close(unit=10,status='keep')



90      if(num.ne.12) goto 560
c       *******************************
c       *    cal. rms & m of patten    *
c       *******************************


c       ***** initialization of the parameter *****
        vol=0
```

111

```
        fir=0.0
        sec=0.0
        s=0          .
        sx=0
        sy=0
        xa=0.0
        ya=0.0


        write(*,405)
405     format(/,t6,'SELECT QUADRANT (0-2)')
        read(*,410)quad
410     format(i2)
        call dquad(quad)
        do 412 i=1,512
        call rowr(i,quad,buf)
        call roww(i,3,buf)
412     continue

c       ***** draw window *****
        call dquad(quad)
        wx1=20
        wy1=10
        wx2=480
        wy2=10
        wx3=20
        wy3=450
        wx4=480
        wy4=450
        wd=5

        call setind(255)
        call moveto(wx1,wy1)
        call lineto(wx2,wy2)
        call moveto(wx2,wy2)
        call lineto(wx4,wy4)
        call moveto(wx4,wy4)
        call lineto(wx3,wy3)
        call moveto(wx3,wy3)
        call lineto(wx1,wy1)

        write (*,426)
426     format(/,t6,'SET THE UPPER LEFT CORNER')
423     continue
        dir=getkey(ii)
```

112

```fortran
      if (dir.eq.274.or.dir.eq.275.or.dir.eq.276.or.dir.eq.277) then
            if (dir.eq.274) then
     .               wy1=wy1-wd
                     wy2=wy2-wd
                     do 431 i=wy1,wy1+5
                     call rowr(i,3,buf)
431                  call roww(i,quad,buf)
            elseif (dir.eq.275) then
                     wy1=wy1+wd
                     wy2=wy2+wd
                     do 432 i=wy1-5,wy1
                     call rowr(i,3,buf)
432                  call roww(i,quad,buf)
            elseif (dir.eq.276) then
                     wx1=wx1-wd*4
                     wx3=wx3-wd*4
                     do 433 i=wx1,wx1+20
                     call colr(i,3,buf)
433                  call colw(i,quad,buf)
            elseif (dir.eq.277) then
                     wx1=wx1+wd*4
                     wx3=wx3+wd*4
                     do 434 i=wx1-20,wx1
                     call colr(i,3,buf)
434                  call colw(i,quad,buf)
            endif

      call setind(255)
      call moveto(wx1,wy1)
      call lineto(wx2,wy2)
      call moveto(wx2,wy2)
      call lineto(wx4,wy4)
      call moveto(wx4,wy4)
      call lineto(wx3,wy3)
      call moveto(wx3,wy3)
      call lineto(wx1,wy1)
            elseif (dir.eq.13) then
      goto 429
      endif
      goto 423

429   continue
      write (*,427)
427   format(/,t6,'SET THE LOWER RIGHT CORNER')
421   continue
```

113

```
        dir=getkey(ii)
        if (dir.eq.274.or.dir.eq.275.or.dir.eq.276.or.dir.eq.277) then
                if (dir.eq.274) then
                        wy3=wy3-wd
                        wy4=wy4-wd
                        do 436 i=wy3,wy3+5
                        call rowr(i,3,buf)
436                     call roww(i,quad,buf)
                elseif (dir.eq.275) then
                        wy3=wy3+wd
                        wy4=wy4+wd
                        do 437 i=wy3-5,wy3
                        call rowr(i,3,buf)
437                     call roww(i,quad,buf)
                elseif (dir.eq.276) then
                        wx2=wx2-wd*4
                        wx4=wx4-wd*4
                        do 438 i=wx2,wx2+20
                        call colr(i,3,buf)
438                     call colw(i,quad,buf)
                elseif (dir.eq.277) then
                        wx2=wx4+wd*4
                        wx4=wx4+wd*4
                        do 439 i=wx2-20,wx2
                        call colr(i,3,buf)
439                     call colw(i,quad,buf)
                endif

        call setind(255)
        call moveto(wx1,wy1)
        call lineto(wx2,wy2)
        call moveto(wx2,wy2)
        call lineto(wx4,wy4)
        call moveto(wx4,wy4)
        call lineto(wx3,wy3)
        call moveto(wx3,wy3)
        call lineto(wx1,wy1)
        elseif (dir.eq.13) then
        goto 422
        endif
        goto 421
422     continue
        ww=int((wx1+wx2)/2.0+0.5)
        write(*,1111)
111     format(/,t6,'Only RMS ?  (Y/N)')
```

```
        read(*,1112)dum
1112    format(a1)

        write(*,428)
428     format(/,t6,'CALCULATING')

c       ***** cal. rms (volume) *****
        do 415 i=wx1+5,wx2-5
        do 420 j=wy1+5,wy3-5
        pr=ipixr(i,j)
420     vol=vol+pr
415     continue
        rmss=vol**0.5
        if (dum.ne.'r') goto 1113
        write(*,425)
425     format('+',t6,'20% FINISHED')


c       ***** cal. center of mass of the patten *****
        do 430 i=wx1+5,wx2-5
        do 435 j=wy1+5,wy3-5
        pr=ipixr(i,j)
        fpr=pr
        fi=i
435     sx=sx+fpr*fi
430     continue
        xa=sx/vol

        WRITE(*,446)
446     FORMAT('+',T6,'40% FINISHED')

        do 440 j=wy1+5,wy3-5
        do 445 i=wx1+5,wx2-5
        pr=ipixr(i,j)
        fpr=pr
        fj=j
445     sy=sy+fpr*fj
440     continue
        ya=sy/vol

        WRITE(*,448)
448     FORMAT('+',T6,'60% FINISHED')

c       ***** cal. 1st & 2nd moment of the patten *****
        do 450 i=wx1+5,wx2-5
        do 455 j=wy1+5,wy3-5
```

```
        pr=ipixr(i,j)
        fpr=pr
        s=6.2831853*((i-xa)**2.0+(j-ya)**2.0)**0.5*1.70333333
        fir=fir+fpr*s
        sec=sec+fpr*s**2.0
455     continue

        IF (I.EQ.ww) THEN
        write(*,458)
458     FORMAT('+',T6,'80% FINISHED')
        ENDIF

450     continue
        write(*,451)
451     format('+',t6,'FINISHED        ')
        write(*,452)
452     format('0',' ')
        fir=fir**0.5
        sec=sec**0.5
1113    continue
        write(*,470) rmss
470     format('0',t6,'      RMS = ',f15.4)
        write(*,460) fir
460     format(/,t6,'1st MOMENT = ',f15.4)
        write(*,465) sec
465     format(/,t6,'    SLOPE = ',f15.4)
        write(*,474)
474     format('0',' ')
        write(*,475)
475     format('0',t6,'PRESS <RETURN> TO CONTINUE')
        read(*,'(a1)') dum


560     if(num.ne.13) goto 101
c       ****************************
c       *     match two images     *
c       ****************************

        do 563 i=1,512
        call rowr(i,1,buf)
        call roww(i,3,buf)
563     continue
        call dquad(1)
        write (*,562)
562     format(/,t6,'QUAD 1 IS NOW ON THE SCREEN')
```

116

```fortran
          m1=70
          n1=325
          CALL SETIND(255)
          call moveto(10,m1+512)
          call lineto(500,m1+512)
          call moveto(500,m1+512)
          call lineto(500,n1+512)
          call moveto(500,n1+512)
          call lineto(10,n1+512)
          call moveto(10,n1+512)
          call lineto(10,m1+512)
          write(*,564)
564       format(/,t6,'SET AREA TO MATCH')
565       continue
          dir=getkey(ii)
          if (dir.eq.274.or.dir.eq.275) then
                  if (dir.eq.274) then
                          m1=m1-5
                          n1=n1-5
                          do 566 i=m1,m1+5
                          call rowr(i,3,buf)
                          call roww(i,1,buf)
566                       continue
                          do 567 j=n1,n1+5
                          call rowr(j,3,buf)
                          call roww(j,1,buf)
567                       continue
                  elseif (dir.eq.275) then
                          m1=m1+5
                          n1=n1+5
                          do 568 i=m1-5,m1
                          call rowr(i,3,buf)
                          call roww(i,1,buf)
568                       continue
                          do 569 j=n1-5,n1
                          call rowr(j,3,buf)
                          call roww(j,1,buf)
569                       continue
                  endif

          CALL SETIND(255)
          call moveto(10,m1+512)
          call lineto(500,m1+512)
          call moveto(500,m1+512)
          call lineto(500,n1+512)
```

```
        call moveto(500,n1+512)
        call lineto(10,n1+512)
        call moveto(10,n1+512)
        call lineto(10,m1+512)
        elseif (dir.eq.13) then
        goto 570
        endif
        goto 565

        tx1='                        '
570     write(*,598)
598     format(/,t6,'TEXT ?')
        read(*,'(a20)') tx1

        do 575 i=m1,n1
        call rowr(i,3,buf)
        j=i-(m1-1)
        call roww(j,0,buf)
575     continue
        call moveto(245,30)
        call setind(255)
        call text(tx1,1)


        do 583 i=1,512
        call rowr(i,2,buf)
        call roww(i,3,buf)
583     continue
        call dquad(2)
        write (*,582)
582     format(/,t6,'QUAD 2 IS NOW ON THE SCREEN')
        m1=70
        n1=325
        CALL SETIND(255)
        call moveto(10+512,m1)
        call lineto(500+512,m1)
        call moveto(500+512,m1)
        call lineto(500+512,n1)
        call moveto(500+512,n1)
        call lineto(10+512,n1)
        call moveto(10+512,n1)
        call lineto(10+512,m1)
        write(*,584)
584     format(/,t6,'SET AREA TO MATCH')
585     continue
```

118

```fortran
               dir=getkey(ii)
               if (dir.eq.274.or.dir.eq.275) then
                       if (dir.eq.274) then
                               m1=m1-5
                               n1=n1-5
                               do 586 i=m1,m1+5
                               call rowr(i,3,buf)
                               call roww(i,2,buf)
586                            continue
                               do 587 j=n1,n1+5
                               call rowr(j,3,buf)
                               call roww(j,2,buf)
587                            continue
                       elseif (dir.eq.275) then
                               m1=m1+5
                               n1=n1+5
                               do 588 i=m1-5,m1
                               call rowr(i,3,buf)
                               call roww(i,2,buf)
588                            continue
                               do 589 j=n1-5,n1
                               call rowr(j,3,buf)
                               call roww(j,2,buf)
589                            continue
                               endif

               CALL SETIND(255)
               call moveto(10+512,m1)
               call lineto(500+512,m1)
               call moveto(500+512,m1)
               call lineto(500+512,n1)
               call moveto(500+512,n1)
               call lineto(10+512,n1)
               call moveto(10+512,n1)
               call lineto(10+512,m1)
               elseif (dir.eq.13) then
               goto 590
               endif
               goto 585
                       tx2='                       '
590            write(*,599)
599            format(/,t6,'TEXT ?')
               read(*,'(a20)') tx2
               do 595 i=m1,n1
               call rowr(i,3,buf)
```

119

```fortran
        j=i-(m1-256)
        call roww(j,0,buf)
595     continue
        call moveto(245,465)
        call setind(255)
        call text(tx2,1)
        call moveto(565,465)
        dum=' '
        call text(dum,1)
        call dquad(0)
        write(*,597)
597     format(/,t6,'DONE !')

101     if(num.ne.14) goto 4
        stop
        end
```

120

VITA AUCTORIS

NAME: Wai-Hong Wong

PLACE OF BIRTH: Hong Kong

YEAR OF BIRTH: 1966

EDUCATION   Pui-Ching Middle School, Hong Kong
1978-1983

Columbia Secondary School of Canada, Hamilton, Ontario
1984-1985

University of Windsor, Windsor, Ontario
1985-1990 B.A.Sc. (Mechanical Engineering)

University of Windsor, Windsor, Ontario
1990-1993 M.A.Sc. (Mechanical Engineering)